OCEAN DRILLING PROGRAM

LEG 168 PRELIMINARY REPORT

HYDROTHERMAL CIRCULATION IN THE OCEANIC CRUST: EASTERN FLANK OF THE JUAN DE FUCA RIDGE

Dr. Earl Davis
Co-Chief Scientist, Leg 168
Pacific Geoscience Centre
Geological Survey of Canada
P.O. Box 6000
Sidney, BC
V8L 4B2
Canada

Dr. Andrew Fisher
Co-Chief Scientist, Leg 168
Earth Sciences Department
University of California, Santa Cruz
Santa Cruz, CA 95064
U.S.A.

Dr. John Firth
Staff Scientist, Leg 168
Ocean Drilling Program
Texas A&M University Research Park
1000 Discovery Drive
College Station, TX 77845-9547
U.S.A.

____
Paul J. Fox
Director
Science Operations
ODP/TAMU

____
James Allan
Interim Manager
Science Operations
ODP/TAMU

____
Timothy J.G. Francis
Deputy Director
Science Operations
ODP/TAMU

October 1996

Preliminary Report No. 68

First Printing 1996

Distribution

Electronic copies of this publication may be obtained from the ODP Publications Home Page on the World Wide Web at http://www-odp.tamu.edu/publications.

D I S C L A I M E R

This publication was prepared by the Ocean Drilling Program, Texas A&M University, as an account of work performed under the international Ocean Drilling Program, which is managed by Joint Oceanographic Institutions, Inc., under contract with the National Science Foundation. Funding for the program is provided by the following agencies:

Canada/Australia/Korea Consortium for the Ocean Drilling Program
Deutsche Forschungsgemeinschaft (Federal Republic of Germany)
Institut Français de Recherche pour l'Exploitation de la Mer (France)
Ocean Research Institute of the University of Tokyo (Japan)
National Science Foundation (United States)
Natural Environment Research Council (United Kingdom)
European Science Foundation Consortium for the Ocean Drilling Program (Belgium, Denmark, Finland, Iceland, Italy, the Netherlands, Norway, Spain, Sweden, Switzerland, and Turkey)

SCIENTIFIC REPORT

The following scientists were aboard JOIDES Resolution for Leg 168 of the Ocean Drilling Program:

Earl Davis (Pacific Geoscience Centre, Geological Survey of Canada, P.O. Box 6000, Sidney, BC V8L 4B2, Canada; E-mail: davis@pgc.emr.ca)

Andrew Fisher (Earth Sciences Department, University of California, Santa Cruz, Santa Cruz, CA 95064, U.S.A.; E-mail: afisher@earthsci.ucsc.edu)

John Firth (Ocean Drilling Program, Texas A&M University Research Park, 1000 Discovery Drive, College Station, TX 77845-9547, U.S.A.; E-mail: john_firth@odp.tamu.edu)

Eva Andersson (Department of Geology and Geochemistry, Stockholm University, S-106 61, Stockholm, Sweden; E-mail: eva.anderson@geokem.su.se)

Kan Aoike (Ocean Research Institute, University of Tokyo, 1-15-1 Minamidai, Nakano-ku, Tokyo 164, Japan; E-mail: bluepond@ori.u-tokyo.ac.jp)

Keir Becker (Rosenstiel School of Marine and Atmospheric Science, Division of Marine Geology and Geophysics, University of Miami, 4600 Rickenbacker Causeway, Miami, FL 33149-1098, U.S.A.; E-mail: kbecker@rsmas.miami.edu)

Kimberly Brown (Scripps Institution of Oceanography, Mail Code 0208, University of California, San Diego, La Jolla, CA 92093, U.S.A.; E-mail: klbrown@ucsd.edu)

Martine Buatier (Laboratoire de Sédimentologie et Géodynamique, Université de Lille I, URA 719 UFR des Sciences de la Terre, F-59655 Villeneuve d’Ascq, France; E-mail: martine.buatier@univ-lille1.fr)

Marc Constantin (Department of Geology, University of Toronto, 22 Russell Street, Toronto, Ontario M5S 3B1, Canada; E-mail: mconstan@quartz.geology.utoronto.ca)

Henry Elderfield (Department of Earth Sciences, University of Cambridge, Cambridge CB2 3EQ, United Kingdom; E-mail: he101@esc.cam.ac.uk)

Carlos Goncalves (LENEP/UENF, Predio da Escola Tecnica, Rod. Amaral Peixoto Km. 164, Imboacica Macae/RJ, 27973-030 BRAZIL; E-mail: carlos@lenep.uenf.br)

Jens Grigel (University Bremen, FB5, P.O. Box 330440, 28334 Bremen, Germany; E-mail: jgrigel@geophys2.uni-bremen.de)

Arlëne Hunter (Department of Earth Sciences, University of Leeds, Leeds, LS2 9JT, United Kingdom; E-mail: a.hunter@earth.leeds ac.uk)

Atsuyuki Inoue (Department of Earth Sciences, Chiba University, Chiba 263, Japan; E-mail: atinoue@earth.s.chiba-u.ac.jp)

Roisin Lawrence (Department of Geology, Duke University, P.O. Box 90229, Durham, NC 27708-0229, U.S.A.; E-mail: lawrence@geo.duke.edu)

Robert Macdonald (Pacific Geoscience Centre, Geological Survey of Canada, P.O. Box 6000, Sidney, BC V8L 4B2, Canada; E-mail: macdonald@pgc.emr.ca)

Pietro Marescotti (Dipartimento Scienze della Terra, Univerità di Genova, C. so Europa, 26 IT 16132 Genova, Italy; E-mail: marescot@dister.unige.it)

Jeffrey Martin (School of Earth and Atmospheric Science, Georgia Institute of Technology, Atlanta, GA 30331-0340, U.S.A.; E-mail: martin@namazu.eas.gatech.edu)

Christophe Monnin (Laboratoire de Géochimie, Université Paul Sabatier, 38 rue des Trente Six Ponts, 31400 Toulouse, France)

Michael Mottl (Department of Oceanography/SOEST, University of Hawaii at Manoa, 1000 Pope Road, Honolulu, HI 96822, U.S.A.; E-mail: mmottl@soest.hawaii.edu)

Daniel Pribnow (Niedersachsisches Landesamt fur Bodenforschung, NlfB-GGA, Stilleweg 2, Hannover, Germany; E-mail: dpribnow@mines.utah.edu)

Joshua Stein (Earth Sciences Department, Earth and Marine Sciences Bldg., University of California, Santa Cruz, Santa Cruz, CA 95064, U.S.A.; E-mail: josh@earthsci.ucsc.edu)

Xin Su (GEOMAR, Christian-Albrechts-Universität, Wischhofstrasse 1-3, Gebaude 4, D24148 Kiel, Germany; E-mail: xsu@geomar.de)

Yue-Feng Sun (Lamont-Dougherty Earth Observatory, Borehole Research Group, Columbia University, Palisades, NY 10964, U.S.A.; E-mail: sunyf@ldeo.columbia.edu)

Michael Underwood (Department of Geological Sciences, University of Missouri, 101 Geology Building, Columbia, MO 65211, U.S.A.; E-mail: geoscmbu@showme.missouri.edu)

David Vanko (Department of Geology, Georgia State University, Atlanta, GA 30303-3083, U.S.A.; E-mail: dvanko@gsu.edu)

Geoffrey Wheat (NURP/MLML Ship Operations, 7700 Sandholdt Road, Bldg. D, P.O. Box 475, Moss Landing, CA 95039-0475, U.S.A.; E-mail: wheat@mbari.org)

ABSTRACT

Ocean Drilling Program Leg 168 investigated three hydrothermal regimes located on the sediment-covered eastern flank of the Juan de Fuca Ridge. The three regimes are (1) a transition from very young (<0.8 Ma) unsedimented igneous crust to sediment-buried crust (0.8-1.2 Ma), (2) an older (~3.5 Ma) area with large topographic relief (>300 m) of igneous crust under a thick (250-600 m) sediment cover, and (3) an intermediate age (1.4-2.6 Ma) area of low relief igneous crust buried continuously over tens of kilometers by sediments averaging about 300 m thick. Ten sites were cored and roughly 1500 m of sediment and basalt was recovered. A total of four CORKs were emplaced, with thermistor strings and osmotic water samplers, in Holes 1024C, 1025C, 1026B, and 1027C. Temperature, pressure, and water chemistry data will be recorded from these holes over the next 3 to 5 years. The first direct sampling of basement fluids in Deep Sea Drilling Project/Ocean Drilling Program history was achieved in Hole 1026B, using the Water-Sampling Temperature Probe (WSTP).

Sites 1023 to 1025 span the hydrothermal transition and show a progressive change in basal sediment pore-water chemistry from normal seawater values with distance from the Juan de Fuca Ridge axis and the area of unsedimented basement. Alteration of basement basalts and upper basement temperatures also increase with distance from the area of outcrop. Slow upflow of pore fluids through the sediment section was detected at Site 1025. Pore-water chlorinity profiles at all three sites suggest that seawater is flowing laterally from the bare igneous crust of the ridge axis eastward through the upper crust, with residence times in basement of perhaps only a few thousand years.

Sites 1026 and 1027 are located only 2 km apart, on a buried basement ridge and basement trough, respectively. Sediment pore-water compositions and upper basement temperatures are similar at both sites (61°-63°C), despite the large difference in sediment thickness (250 vs. 600

m). Fluid flow in basement is, thus, inferred to be sufficiently vigorous to maintain relatively uniform temperatures at the sediment/basement interface. Direct sampling of basement pore water from Hole 1026B shows that some elemental concentrations are quite different from those measured in the basal sediment interstitial water, indicating significant reaction in the basal sediments. The basement pore waters are similar to those expelled from nearby basement outcrops, indicating a high degree of compositional homogeneity, which is consistent with the temperature data. Basement pore waters flowing up through Hole 1026B were about 2°-3°C warmer than the temperature at the sediment/basement interface. This indicates that the first zone of high permeability is somewhat deeper than the sediment/basement interface.

Sites 1028, 1029, and 1032 form a transect perpendicular to the ridge axis, across a broad area with low-relief ocean crust that was thought to be relatively isolated from the overlying ocean by a continuous blanket of sediments 200-300 m thick. Sites 1028, 1029, and 1032 were designed to measure basement temperatures in order to calculate regional lithospheric heat flux and to allow determination of basement fluid compositions over a range of temperatures. Basement basalts at these sites all show an initial stage of oxidative alteration, requiring significant open seawater circulation, followed by subsequent alteration representing relatively closed hydrothermal circulation. Pore-water geochemistry shows evidence for incompletely evolved seawater in the basement. Basement temperatures at these sites are much lower than would be expected (51°-59°C), if the crust was fully sealed from exchange of hydrothermal fluids with the ocean. This, and the basement-water compositions, indicate that there is significant lateral transport of basement fluids, and advective heat loss, over much greater distances than previously thought.

Sites 1030 and 1031 were drilled to investigate a local geochemical anomaly on a shallow (<50-m sediment) buried ridge. High chlorinity values and other elemental concentrations in the sediment pore waters may indicate a deeper reaction zone and/or a longer residence time in basement for these fluids, in contrast to sites drilled to the east and west. Pore-fluid chemical profiles indicate an upward flow of pore waters through the sediment section at these thinly sedimented sites.

BACKGROUND

While the most spectacular manifestation of oceanic crustal fluid circulation is high-temperature

(350°-400°C) venting along mid-ocean-ridge axes, a much greater flux of hydrothermal heat and seawater occurs within the igneous crust along ridge flanks, well away from spreading centers. Modeling and observations of heat flow indicate that advective heat loss through ridge flanks is globally more than triple that at ridge axes, and because this heat is advected at lower temperatures, the volumetric flux of seawater through the flanks is proportionately even greater, perhaps more than 10 times that at the axes. Significant hydrothermal heat loss and fluid exchange between the crust and ocean typically continue to an age of several tens of millions of years and, thus, effect more than one-third of the ocean floor. This process plays an important role in the alteration of oceanic crust, which includes changes in its chemistry, mineralogy, and physical properties such as seismic velocity and attenuation. However, because of the wide range of conditions on ridge flanks and the limited amount of work done there to date, we know little about these processes in detail. Major questions remain: what mechanisms drive fluid flow through the crust and seafloor, what is the magnitude of elemental chemical exchange between the crust and water column, and what factors are most important in influencing water/rock interactions and, thus, in controlling fluid chemistry and the chemical and physical alteration of the igneous crust and its sediment cover?

Over the past two decades, several sites of hydrothermal circulation on mid-ocean-ridge flanks have been investigated. These include the Galapagos mounds, the southern flank of the Costa Rica Rift, the equatorial East Pacific Rise flank, the western flank of the East Pacific Rise near 20°S, the western flank of the Mid-Atlantic Ridge, and the flank of the Mariana Trough spreading axis. These sites represent a wide range in sediment thickness and continuity, sediment type, crustal age, and basement topography. Although these localities display a correspondingly wide range of hydrothermal conditions and processes, our understanding of the processes remains only semiquantitative.

As a result of a series of coordinated surface-ship and submersible studies that began with a reconnaissance survey in 1988, the eastern flank of the Juan de Fuca Ridge has become one of the most thoroughly studied ridge flanks. By providing critical hydrologic, geophysical, and geochemical samples and observations of three characteristic types of subseafloor fluid-flow systems (Hydrothermal Transition [HT] system from bare crust to sedimented crust; Rough Basement [RB] system with basement topography influencing fluid flow; and Buried Basement

[BB] system with "flat" basement covered by sediment) that occur in simple form on this ridge flank, work conducted during Ocean Drilling Program (ODP) Leg 168 will greatly improve our understanding of ridge-flank hydrothermal circulation and crustal evolution.

GEOLOGICAL SETTING

The Juan de Fuca Ridge is a seafloor-spreading center several hundred kilometers off the coast of North America (Fig. 1). It is creating the crust and lithosphere of the Juan de Fuca plate at a rate of about 29 mm/yr. The topographic relief of the ridge produces a barrier to terrigenous turbidite sediment supplied from Pleistocene glacial sources along the continental margin, primarily at Queen Charlotte Sound, Juan de Fuca Strait, and the Grays Harbor and Columbia River estuaries. This situation has resulted in the accumulation of an onlapping layer of sediment that buries the eastern flank of the Juan de Fuca Ridge. This sedimented region known as the Cascadia Basin, extends from the base of the continental margin, where accretion of the sediment entering the Cascadia subduction zone begins, to within a few tens of kilometers of the ridge crest, where sediment laps onto crust that is younger than 1 Ma at some locations (Fig. 2). Along the deformation front of the northern Cascadia accretionary prism the sediment layer is more than 3 km thick; in the northern part of the basin, the fill is sufficient to completely bury most of the relief of the igneous crust of the Juan de Fuca plate. The local basement relief beneath the nearly continuous, flat-lying sediment cover is dominated by linear ridges and troughs that were produced by normal faulting and variations in volcanic supply at the time the crust was created. The amplitude of this relief varies across the basin, from less than 100 m in places to over 700 m in others with the exception of only a few isolated volcanic cones and seamounts (see Leg 168 Scientific Prospectus). A few of these penetrate the sediment section.

HYDROTHERMAL TRANSITION TRANSECT (SITES 1023, 1024, AND 1025)

Setting of the Hydrothermal Transition Transect

A fundamental change in the nature of hydrothermal circulation occurs as sediment thins between the ridge crest and the low basement ridges that approach the seafloor 20 km to the east of the ridge. Within 20 km of the ridge, basement is exposed to the overlying ocean or covered by a relatively thin (less than 1 m to a few tens of meters), discontinuous veneer of hemipelagic sediment through which fluids can pass with little hydrologic impedance. To the east of this area of extensive igneous outcrop, the igneous crust is blanketed continuously by turbidite sediments that create a hydrologic barrier. Heat flow and estimated upper crustal temperatures, seismic velocities in the upper crust, and estimates of basement pore-fluid compositions all indicate lateral gradients associated with the transition from open to sealed hydrothermal circulation. Heat flow and estimated basement temperatures increase systematically to the east, away from the area of exposed basement. Estimated temperatures in the upper igneous crust increase from less than 10°C near where basement rocks outcrop to about 40°-45°C another 20 km to the east (40 km from the ridge). Over this same distance the average heat flow increases from less than 15% to more than 80% of the value expected for the underlying lithosphere.

Basement pore-fluid compositions, estimated from sediment pore-fluid studies, are close to seawater at 20 km from the ridge, but are strongly depleted in magnesium and enriched in calcium at 40 km from the ridge. The basement fluids 20 km east of the point of burial have considerably higher inferred chlorinities than seawater. Part of the increased chlorinity may be due to ongoing hydration reactions in the crust. This is consistent with the increase in basement temperature and with the seismic data, which also reveal a systematic change. Interval velocities determined for the upper crustal seismic Layer 2A increase from values ranging from 3000-3500 m/s to values exceeding 5000 m/s over the same spatial interval of about 20 km. Although these velocities were determined for a layer known to have strong vertical velocity gradients, they probably indicate a significant increase in velocities throughout Layer 2A. The increase is believed to indicate a decrease in porosity and bulk modulus resulting from alteration. A similar magnitude of change occurs on other ridge flanks, although at a much slower rate, probably because the hydrologic isolation of the upper igneous crust is normally much more gradual.

Goals of the Hydrothermal Transition Transect

To document changes in basement fluid temperatures and compositions, the physics of fluid flow, and alteration of the crustal rocks, a transect of holes was completed across this hydrothermal transition. Drilling was directed toward solving numerous fundamental questions about lateral fluid and heat transport and about the physical and chemical alteration of the crust that results from water/rock interaction. Specific questions include the following:

1. How does chemical and thermal transport take place over distances of 10-20 km in sediment-covered igneous crust? If there is a net horizontal transport of fluid, what is the rate?
2. What is the source and magnitude of the pressure gradient that drives the flow?
3. How do the changes in fluid chemistry and temperature with distance from sediment-free areas affect the nature of rock alteration?
4. What is the dominant factor responsible for the increase in upper crustal velocity?
5. Is there an accompanying decrease in permeability?
6. At what rate does the alteration take place?

It was anticipated that if relationships could be determined between basement temperature, fluid chemistry, and crustal alteration, then the results of studying this simple hydrothermal transition zone could be generalized to other ocean basins.

Scientific Results

Drilling at Sites 1023, 1024, and 1025 (Fig. 3) recovered similar sequences of rhythmic sand and silt turbidites (lithologic Unit I) (Fig. 4). Most individual beds are a few centimeters to 1 m thick and are interbedded with hemipelagic mud typically tens of centimeters to 1 m thick. These sequences were deposited above an interval of turbidite-free hemipelagic mud, ranging from 3 to 20 m thick (Unit II), which was, in turn, deposited directly over igneous basement (Unit III). The total thickness of Unit I is 190, 150, and 87 m at Sites 1023, 1024, and 1025, respectively. Calcareous nannofossils sampled from the hemipelagic layers show the following age correlations: base of *Emiliania huxleyi* (~0.28 Ma) at roughly 43 meters below seafloor (mbsf) (Site 1023), 30 mbsf (Site 1024), and 34 mbsf (Site 1025); top of *Pseudoemiliania lacunosa* (~0.46 Ma) at base of sediments (192.46) mbsf at Site 1023; and Site 1025 does not contain *P. lacunosa*, thus the basal sediments are <0.46 Ma. Site 1024 contains the Brunhes/Matuyama magnetic polarity reversal (0.78 Ma) at 166.2 mbsf. Basement ages of

Sites 1023, 1024, and 1025 from seasurface magnetic anomalies are 0.87, 0.99, and 1.27 Ma, respectively, which indicates that sedimentation did not begin for several thousand years after basement formation.

Basement was intersected at 192.8, 167.8, 97.5 mbsf, in Holes 1023A, 1024B, and 1025B, respectively. In Holes 1023A, 1024B, and 1025B, 1 m of basement was cored in each hole with the extended core barrel (XCB) coring system and 6 to 16 unoriented pieces of fragmented pillow basalt were recovered. Basement was also recovered from reentry Holes 1024C and 1025C. Rotary core barrel (RCB) coring in Hole 1024C penetrated only 2 m and produced 6% recovery, whereas coring in reentry Hole 1025C extended from 106.1 to 147.2 mbsf and recovery was 36.9%.

Recovery from the XCB holes yielded many basalt pieces with thin unaltered glass rims. Phenocryst contents (plagioclase, olivine, and clinopyroxene) vary 1%-2% in the basalt from Hole 1023A but <1% in the aphyric basalt from Holes 1024B and 1025B. All the basalt is vesicular (<1% vesicles, diameters <1 mm). Two types of volcanic units were identified from RCB coring of the reentry holes: pillow lava and massive basalt. Pillow basalts occur in Hole 1024C. A succession of massive basalts (the total recovery from Hole 1025C) occurs structurally below the Hole 1025B pillows. Rare glass rims (separated by about 1 to 15 m) occur in the massive basalt units. Phenocryst contents are <1% plagioclase plus clinopyroxene phenocrysts in the aphyric basalts sampled in Hole 1024C and the massive basalt from Hole 1025C. The plagioclase phenocrysts range in size up to 5 mm long, whereas the mafic phenocrysts are generally ≤1 mm in diameter. The pillow basalts have <1% vesicles. The massive basalts have variable vesicularity, up to 12%, and are moderately altered (5%-25%).

Whole-rock major-element analyses show the basalts from Site 1024 are low-K tholeiites with $Mg/(Mg + Fe^{2+}) * 100$, or Mg#, of 60-62, whereas, those from Site 1025 are ferrobasalts (Mg# = 46-49) with TiO_2 equal to 2.43 to 2.70 wt% and Fe_2O_3 equal to 14.50 to 15.91 wt% (with all iron calculated as Fe_2O_3). These Site 1025 rocks are the most fractionated rocks known from the Endeavour segment of the Juan de Fuca Ridge.

All basement rocks from Sites 1023, 1024, and 1025 exhibit alteration, which is manifested in several ways and varies between sites. The presence of fresh olivines in Hole 1023A indicates that these samples have undergone the least amount of alteration. In contrast to Hole 1023A, practically all olivines from Site 1025 are completely replaced by a mixture of clay minerals (primarily saponite with some celadonite), minor carbonate, and rare talc and chlorite/smectite. Sample interiors vary from fresh (defined as <2% replacement by alteration minerals) in most of the pillows to slight tomoderate (5%-25% alteration minerals) in the massive ferrobasalts.

Many pieces from Site 1024 contain centimeter-scale alteration halos just inside their outer surface. In hand specimen these halos have orange, yellow, and dark green material filling the vesicles. Microscopic observations suggest that these vesicle fillings include celadonite, saponite, and iron oxyhydroxides. Halos are rare in rocks from Hole 1023A and Site 1025.

Nearly all basement samples from Sites 1023, 1024, and 1025 possess incomplete clay coatings on their outer surfaces. The clay minerals are usually a light blue to blue-green color in hand specimen, and X-ray diffraction indicates that these clays are trioctahedral smectites. In nearly all basement samples from Sites 1023, 1024, and 1025, the vesicles (excluding those within alteration haloes) are completely lined by a fine-grained blue clay, which is probably the same as that observed on the sample surfaces. In microscopic sections, this mineral is identified as saponite. Some basement samples from Sites 1023, 1024, and 1025 exhibit zeolites associated with the blue clay mineral on rock surfaces and within vesicles. Pyrite occurs as a trace mineral associated with saponite on many basement pieces and inside vesicles from all HT sites. Several vein types occur at Site 1025; 111 veins were logged in Hole 1025C, including: clay (90 veins), clay + talc (10), clay + carbonate (6), clay + pyrite (1), talc (1), and quartz + clay (3). Most veins are ≤1 mm wide.

Basalts from the HT transect illustrate progressive changes in alteration intensity related to increasing basement temperature from Sites 1023 to 1024 to 1025 and variations in lithology. Higher basement temperatures and coarser grain sizes combine to produce larger degrees of hydrothermal alteration, from a fraction of 1% in aphanitic pillow basalts that have a temperature of 15.5°C, up to 25% alteration in fine-grained massive basalts in basement that have a temperature of 38.2°C at the basement/sediment interface. There is no evidence from the alteration features that these rocks ever experienced higher temperatures than those measured on this leg.

Methane is the dominant volatile hydrocarbon gas in the cored sediments and shows a strong negative correlation with pore-water sulfate concentrations at all sites. Sedimentary organic matter is low in organic carbon and has C/N ratios indicating a predominately marine origin. The organic matter is hydrogen poor, reflecting selective degradation of less stable marine organic compounds.

The composition of pore water at the three sites shows clear indications of reaction and diffusion in the sediment section. Vertical advection was evident only in Hole 1025B, where slow upward seepage of water is indicated by a systematic variation in profiles of Ca, Mg, and alkalinity (Fig. 5). Some degree of superhydrostatic pressure in basement at this site was also indicated by the presence of discharge from Hole 1025C, which was drilled through the sediments and ~5 m into upper basement. This was seen with the vibration-isolated television (VIT) camera at the time of reentry with the 10-3/4" casing string.

Basement-water compositions, inferred from pore-fluid compositions in basal sediments, reveal systematic changes with increasing temperature and distance from the outcrop in some elemental concentrations. Changes are most apparent in magnesium and calcium, which are particularly reactive in basement. Concentrations at Hole 1023A were 48-mM Mg and 12-mM Ca, only slightly different from seawater at 53-mM Mg, and 10.6-mM Ca. At Site 1025, the site farthest from outcrop, Mg fell to 28 mM and Ca rose to 37 mM. Chlorinity values are perhaps most interesting. The commonly observed increase from present-day seawater values of 555 mM at the seafloor to elevated values of relic Pleistocene water at depths of a few tens of meters below seafloor was seen at all three sites. Values decreased at greater depths, however, back to values identical to present-day seawater in Holes 1023A and 1024B and to only a slightly elevated value (560 mM) in Hole 1025B. A simple interpretation of these low chlorinity values is that the water has a residence time in basement of only a few thousand years, even at the site most distant from outcrop.

Sediment physical properties along the Hydrothermal Transition Transect generally reflect increasing compaction with depth and variations in sand, silt, and clay contents. Finer grained sediments exhibit a consistent decrease in porosity and increase in bulk density with depth, whereas coarser grained units do not. Sediment thermal conductivities are dominated by differences in sand content and in the finer grained parts of the section by compaction .

Sediment magnetic susceptibility was measured continuously with the multisensor track (MST). This permitted the identification of sandy layers in cores before they were split, facilitating the collection of whole-round samples for later permeability and thermal conductivity analyses. The massive basalts recovered from Hole 1025C have porosities below 10 vol%, *P*-wave velocities above 5 km/s, and thermal conductivities of about 1.8 W/m/K.

Temperatures were measured in the sediment section with the goal of obtaining accurate determinations of the temperature of the sediment/basement interface, which is inferred to be a primary hydrologic contact between the low-permeability sediment cover and high-permeability extrusive igneous rocks beneath. Temperatures at the contact increased systematically with distance from the region of outcropping basement, from approximately 15.5°C at Hole 1023A, to 22.4°C at Hole 1024B, and to 38.2°C at Hole 1025B (Fig. 6). All temperature-depth profiles are approximately linear, indicating conductive heat transport through the sediment column.

Holes 1024C and 1025C were designed as reentry CORK holes. These holes were cased and cemented into basement. After curing, the cement at the base of casing was drilled out, and additional coring and drilling were continued into basement. Permeablility measurements of upper basement were attempted by setting the drillstring packer in casing in Hole 1025C, but the packer could not be set and no data were obtained. Packer measurements were successfully completed in basement in Hole 1024C, however, and preliminary examination of the data suggests that basement at this site is relatively permeable. The consistency of basement lithologies and drilling difficulties between Sites 1024 and 1025 suggest that upper basement in Hole 1025C is also permeable.

Instrumented CORK systems were deployed in both Holes 1024C and 1025C (Fig. 7). Each instrument package comprises a long-term data logger, two absolute pressure gauges (one for sealed-hole pressures and one for seafloor pressures), a continuously operating osmotic fluid sampler, and 10 thermistor temperature sensors, including several thermistors positioned within basement in each hole. The first data from these instruments will be retrieved during summer 1997 using the remotely operated vehicle *Jason*.

ROUGH BASEMENT TRANSECT
(SITES 1026 AND 1027)

Setting of the Rough Basement Transect

It has long been believed that basement topography and local basement outcrops play a key role in seafloor hydrogeology enhancing buoyancy-driven flow and focusing flow from the igneous crust into the oceans. One hundred kilometers east of the Juan de Fuca Ridge axis, locally rugged igneous crust is nearly completely buried by sediments, providing an ideal area for studying this process. Basement topography consists primarily of linear ridges and troughs produced by axial block faulting and volcanism. Local relief between ridges and troughs of 300 to 500 m is common, and major ridges are separated typically by 3-7 km. Sites 1026 and 1027 are located over 3.5-Ma crust in this region of rough basement topography (Fig. 2), near where three small basement outcrops penetrate the sediments that otherwise bury basement. At these outcrops, exposure of permeable igneous rocks to the overlying ocean permits crustal water to discharge at the seafloor.

Sites 1026 and 1027 are separated by 2.2 km along a line perpendicular to the strike of basement structure (Fig. 3), about 6 km from the closest and smallest of the basement outcrops. Site 1026 is located over the crest of a buried linear basement ridge where the sediment thins to 230-250 m. Site 1027 was drilled into an adjacent buried valley, where the sediment thickness reaches more than 600 m.

The simplicity of the local structure and the small size of the volcanic outcrops on this part of the east flank of the Juan de Fuca Ridge make the area an ideal target for seafloor studies. Results of a series of systematic predrilling surveys established several aspects of the fluid flow and discharge system:

1. Fluid circulation within the upper oceanic crust is sufficiently vigorous to maintain relatively uniform temperatures at the sediment/basement interface, despite variations of sediment thickness of more than a factor of 5.
2. In the few locations where samples could be obtained, basement-fluid compositions also appear locally homogeneous.

3. Fluids leak through the sediment "seal" above buried basement ridges at geochemically detectable rates (<1 mm/yr to tens of millimeters per year) that are inversely proportional to the local sediment thickness.
4. Fluids flow through the basement outcrops at rates sufficient to produce warm springs at the seafloor and to generate detectable thermal, chemical, and light transmissivity anomalies in the water column. The total advective heat loss is inferred to be great enough to cause the heat flow in the vicinity of the outcrops to be depressed substantially below the level expected from this 3.5-Ma lithosphere.
5. Discharge through the outcrop has been sufficiently long-lived to allow significant hydrothermal precipitates to accumulate. Cores recovered from the outcrop have been composed of green clay, semilithified black ferromanganese crusts and layers, and reddish iron oxides in indurated sediment.
6. The thermal structures of all three basement outcrops are fundamentally the same, allowing us to conclude that upflow and discharge not only are stable and long-lived, but also are a general consequence of the permeability and temperature structure of what we have referred to as "Permeable Penetrators" in the Scientific Prospectus.

Although the complete burial of the ridges and nearly complete burial of the outcrops in this area make them exaggerated examples, they are representative of a general class of circulation that is present wherever the crustal topographic relief of mid-ocean-ridge flanks is partially or completely filled in by sedimentation. An example of an "early" phase of this ridge type is the region of North Pond on the Mid-Atlantic Ridge flank. A relic, fully buried example was probably intersected at Site 417 on the Mid-Atlantic Ridge flank. A highly focused and very active example was investigated during Leg 139 in the Middle Valley rift.

Examples of topographically influenced circulation within the upper igneous crust occur on the Costa Rica Rift flank (holes in the vicinity of and including Hole 504B) and possibly on the northern flank of the Galapagos spreading center. Again, the high degree of burial makes the Juan de Fuca Ridge flank an exaggerated example of topographically influenced fluid flow, but one that is ideally suited to the study conducted during Leg 168.

Goals of the Rough Basement Transect

Primary objectives at this pair of sites included documenting precisely the lateral gradients in basement-fluid temperature, pressure, and composition to constrain the rates of fluid flow in the uppermost igneous crust; estimating the history of fluid flow in basement and through the sediment section; and determining the degree of hydrothermal alteration of the oceanic crust in this environment. Specific questions include the following:

1. To what degree are basement fluids thermally and chemically homogenized by circulation in this environment?
2. What implications can be drawn about the bulk hydrologic transport properties of the upper crust from constraints gained from observations of lateral temperature, pressure, and compositional gradients?
3. How is permeability distributed within upper basement?
4. To what degree has hydrothermal alteration of the crust proceeded at this 3.5-Ma site, and how has the alteration proceeded with time and burial history?
5. How have physical properties, namely seismic velocity and permeability, changed with alteration?
6. What are the nature and magnitude of the forces that drive fluid flow through the sediment section above basement ridges and through Permeable Penetrators where basement is exposed at the seafloor?
7. What is the source of the fluids that vent through the seafloor at the outcrops? Do they simply come from the inferred homogeneous basement "reservoir" regionally sealed beneath the sediments or is there a component from a deeper source?
8. How are sediments chemically and physically affected by fluid seepage? Can a declining rate of seepage through the sediment section be tracked through the history of burial?
9. What is the nature of recharge? Is seawater supplied to the crust solely by regional diffuse flow through the sediments away from basement highs or do some fluids enter the crust via locally focused pathways through basement?

Scientific Results

Shallow sediment cores recovered from both sites contain interbedded sand turbidites, silt turbidites, clayey silt, and debris-flow deposits with clasts of mud in a matrix of muddy sand. This mixture of sediments was designated lithologic Unit I at Site 1026 (Fig. 8). Interlayered sediments of the same types were designated subunit IA at Site 1027, where they extend to 184 mbsf. Subunit IB at Site 1027 comprises interbeds of silt turbidites within clayey silt and silty clay, extending from 184 to 467 mbsf. The sandy intervals in Unit I were found to be thicker at Site 1027 than at Site 1026, both in recovered cores and as inferred for a large depth interval that yielded little or no recovery in Hole 1027B. This contrast in thickness is consistent with the local seismic structure, which shows Site 1027 located approximately in the center of a broad distributary channel and Site 1026 near the edge where the channel fill onlaps a levee of a neighboring channel system. Despite the poor recovery in sandy intervals, hole conditions in Hole 1027B remained surprisingly good down to basement. Recovery improved substantially below 260 mbsf and remained generally high until basement was reached. Lithologic Unit II was hemipelagic mudstone with variable calcium carbonate content. This unit extends from 467 to 569 mbsf in Hole 1027B. The base of Unit II coincides with the first appearance of basalt within thin interbeds of pelagic and hemipelagic mudstone. Sediment alteration was not discernable with shipboard determinations of bulk mineralogy except in the sections a few meters above basement. The most obvious signs of alteration occur in carbonate-rich sediment in immediate contact with basement. In Hole 1027C, the basal sediments displayed vivid color variations imparted by Fe-Mn oxides.

Species diversity of nannofossils at Sites 1026 and 1027 is low, although a few key species provided some age control. *E. huxleyi* (0.28 Ma) was identified throughout the 101-m interval drilled in Hole 1026A; the base of this zone was found at about 98 mbsf in Hole 1027B. Other age controls in Hole 1027B include the top of *P. lacunosa* (~0.46 Ma) at 197 mbsf, the top of *Calcidiscus macintyrei* (~1.58 Ma) at 282 mbsf, and the base of *Gephyrocapsa lumina* (~1.68 Ma) at 417 mbsf. The dominance of *Reticulofeuesta minuta* and *R. minutula* in the assemblage below 417 mbsf, as well as the absence of *R. pseudoumbilicus*, suggests an age of late Pliocene for these deeper sediments including those interbedded with the basalt fragments at the bottom of the hole. These ages are consistent with sea-surface magnetic anomalies that constrain the age of basement at 3.47 and 3.55 Ma at Sites 1026 and 1027, respectively. All age constraints are consistent with an increasing sedimentation rate through the history of basement burial.

Hard rock was first drilled in Hole 1026B at 247.1 mbsf (Fig. 9). The first cored basalt recovered from Hole 1026B was from 256.0 mbsf, with basement coring continuing to a depth of 295.2 mbsf for a total of 39.2 m. Total recovery was 5.0%. Coring of basaltic rocks in Hole

1026C commenced where drilling first encountered basement at 228.9 mbsf. Two cores were cut to a total depth of 248.2 mbsf for a total of 19.3 m; total recovery was only 3.5%.

At Site 1027, basalt was recovered during XCB coring where drilling first encountered basement at a depth of 568.3 mbsf in Hole 1027B. After 9.6 m of basement was cored at Hole 1027B, Hole 1027C was begun with the objective of casing into basement and then coring farther below the cemented casing shoe for a CORK installation. In Hole 1027C, diabase was first recovered from 584.8 mbsf, or 9.3 m below the first hard rock felt by the drillers at 575.5 mbsf, and coring continued an additional 47.6 m. Core 168-1027C-1R consisted of diabase, whereas, Core 168-1027C-2R and most of Core 168-1027C-3R contained terrigenous clay and pelagic sediments. The last 28 cm of Core 168-1027C-3R and all of Cores 168-1027C-4R and 168-1027C-5R contained fractured pillow basalts. Total recovery was 10% in the XCB core from Hole 1027B, 73% in a massive diabase unit from Core 168-1027C-1R, 36% and 73% in fractured pillow basalts from Cores 168 1027C-4R and 168-1027C-5R, respectively.

The basaltic rock types recovered at the two Rough Basement sites vary significantly. The rocks from Hole 1026B are divided into three units. Unit 1 comprises slightly to moderately altered aphyric plagioclase-pyroxene basalt. Unit 2 is a highly altered basalt-hyaloclastite breccia, and Unit 3 consists of a slightly to moderately altered aphyric basalt and moderately phyric pyroxene plagioclase-olivine basalt. All three units exhibit sparse, thin glass margins, with all basalts containing sparse (<1%), small (<1 mm diameter) vesicles. The rocks may represent a complex of pillow basalts and interpillow basalt-hyaloclastite breccia. Hole 1026C consists of pillow basalts, designated Unit 1; these are also sparsely phyric, slightly to moderately altered basalts with several occurrences of glassy margins.

At the deeper basement site (Site 1027), four distinct units were identified. In Hole 1027B, Unit 1 is a massive aphyric olivine-plagioclase-pyroxene basalt with slight to moderate alteration. Unit 2, separated from Unit 1 by at least 15 cm of hemipelagic or pelagic carbonate-bearing mud, is a basaltic breccia containing fragments of basalt similar to that of Unit 1. The first rock cored in Hole 1027C is Unit 3, which is a fine-grained plagioclase-olivine-pyroxene diabase with an aphanitic lower chilled margin; the upper margin was not sampled. Alteration varies from slight to moderate between the diabasic core and the aphanitic margin. Below Unit

3 is at least 10.6 m (23.0 m according to the driller's record) of terrigenous clay and bedded, altered and deformed carbonate-rich pelagic sediments. Consequently, Unit 3 is interpreted as a sill that was emplaced off-axis. The final 19 m of coring in Hole 1027C recovered portions of a pillow basalt sequence, recognized by abundant glassy chilled margins (every 0.6-1.2 m, on average). These pillow basalts are slightly to moderately altered, aphyric to moderately phyric plagioclase-olivine and plagioclase-olivine-pyroxene basalts. All four igneous units from Site 1027 contain sparse (<1%), small (<1 mm diameter) vesicles.

Major-element X-ray fluorescence analyses show all the rocks to be low-potassium tholeiitic basalts with variable Mg#. The diabase of Hole 1027C and the massive basalts of Hole 1027B, however, differ significantly from the pillow basalts from Holes 1027C, 1026B, and 1026C. The pillow basalt geochemistry defines well-constrained linear variation diagrams, suggesting that these basalts may be related through simple low-pressure fractionation of olivine, plagioclase, and/or clinopyroxene. In contrast, the diabase and Hole 1027B massive basalts have chemical compositions very similar to each other, which lie off the fractionation trends defined by the pillow basalts. This suggests that the two distinct chemical groups represent different magmatic events. The pillow basalts were probably erupted in an axial or near-axial environment, whereas the diabase and massive basalts must have erupted onto or intruded into the sediment section at a later stage at an off-axis location.

Alteration effects in basalt from Sites 1026 and 1027 vary significantly between igneous units, although certain features are ubiquitous. Nearly all samples contain mineral linings or complete mineral fillings of vesicles. Typically, the vesicle filling involves two to four sequential layers. The observed distribution of the various vesicle fills is systematic and is linked to the proximity of the vesicles to veins and alteration halos. In addition, we observed veins and mineral coatings on fractured rock surfaces. A third mode of alteration is the replacement by clays of magmatic phases including phenocrysts, groundmass crystals, cryptocrystalline mesostasis, and glass.

In summary, petrological studies at Sites 1026 and 1027 suggest the presence of two distinct magmatic series with distinct alteration histories. Pillow basalts from Site 1026 and from the deepest cores at Site 1027 represent petrogenetically related mid-ocean-ridge basalts with abundant early oxidative alteration, which is probably the result of extended exposure of the rocks at the seafloor. In contrast, the diabase and the massive basalts from Hole 1027B and the first core of Hole 1027C are petrogenetically distinct from the pillow basalts and represent the products of off-axis magmatism; these rocks did not experience significant oxidative alteration by seawater. Finally, an overprint of calcium carbonate alteration affects all of the rocks at Site 1027, whereas calcium carbonate is only a minor alteration product at Site 1026. The reason for this difference may relate to the location of Site 1026, drilled into a buried ridge, and Site 1027, in a buried valley, and consequent differences in the hydrothermal regime.

Profiles of inorganic pore-water composition at the two sites follow similar trends and reflect reaction with sediments, flow of incompletely altered waters in basaltic basement, water/rock reactions in basement, and temporal variations in the composition of bottom water from glacial and interglacial periods. Although the chemical data do not indicate significant flow of pore fluids vertically through the sediments, when Hole 1026B was reentered immediately before deploying the CORK in that hole, temperatures within the borehole indicated that basement water was flowing from the formation into the hole, and then up through the casing and into the overlying ocean. Basement fluid pressure at this location must therefore be locally superhydrostatic, but the low permeability of the sediment section must limit natural fluid seepage to a rate below that geochemically detectable. The water sampler temperature probe was run into the hole to collect a sample of the discharging basement fluid and to log temperatures in the borehole so the fluid velocity could be estimated. This was the first successful sampling of true basement fluid in the history of the Deep Sea Drilling Project (DSDP) and ODP. The sample was sufficiently large to allow post-cruise carbon-14 analyses to determine the age or a limiting age of the hydrothermal fluid. To a first order, this basement fluid has the same composition as the fluid exiting from the nearest basement outcrop that was sampled by submersible. It differs in several notable respects from the composition suggested by interstitial-water samples collected from sediments just above basement (Fig. 10). Methane concentrations increased from near zero near the seafloor and basement to values on the order of 10^4 ppm by volume in the middle of the sediment section at Sites 1026 and 1027. Ethane also was present at low concentrations in headspace samples. Pentane and minor light alkene hydrocarbon gases (<1 ppm) were present at 360 mbsf at Site 1027. The methane/ethane ratio decreased from 26,000 at 200 mbsf to 900 at the base of the sediment section.

Physical properties measurements within the sediment section revealed the expected effects of consolidation and lithification with depth, with local variations associated with changes in sand, silt, and clay contents. *P*-wave velocities measured in the laboratory at atmospheric pressure were near 1.5 km/s at the seafloor and increased to 1.7 to 1.9 km/s near basement. Velocities of the mudstone in lithologic Unit II were found to be anisotropic, with horizontal velocities higher than vertical. MST magnetic susceptibility and gamma-ray attenuation porosity evaluator (GRAPE) data allowed rapid delineation of fining-upward turbidite sequences, as well as relatively homogeneous sandy intervals (where these were recovered) before the core was split, facilitating the selection of whole-round physical properties samples collected for shore-based studies.

As at the previous sites, temperatures were measured in the sediment section with the goal of obtaining accurate determinations of temperature of the sediment/basement interface, which is inferred to be a primary hydrologic contact between the low-permeability sediment cover and high-permeability extrusive igneous rocks beneath. At Site 1026, the temperature at the contact estimated by extrapolation of advance hydraulic piston corer (APC) and Davis/Villinger Temperature Probe (DVTP) measurements is approximately 61°-62°C, only slightly lower than at the extrusive contact at Site 1027, about 63°C (Fig. 11). These temperatures represent only lower limits for those of "hydrologic basement," because the first zone of high permeability at any given location will probably lie deeper than the sediment/basement contact. This is illustrated well by the lack of agreement between the sediment/basement contact temperature estimated at Site 1026 (~61°-62°C) and the measured temperature of discharging basement water (~64°C). Uncertainties of this magnitude preclude resolving whether hydrothermal temperatures are systematically warmer at the ridge or the valley. Resolution of this question should be possible following the examination of data from the long-term CORK installations at these sites. At this time it can be concluded only that upper basement temperatures are uniform to within a few degrees.

Successful packer experiments were conducted in both Holes 1026B and 1027C. The packer was first set in casing at the base of Hole 1026B. Basement pressures recorded while the packer element was inflated (isolating the open hole) indicated a slight underpressure after correction for the cold hydrostatic water column in the borehole, although later flow from the formation into the borehole indicated the formation is naturally overpressured. The retention of a basement underpressure at the end of the Hole 1026B packer tests suggests that the CORK experiment should allow accurate determination of ambient basement fluid pressures. The two slug tests are consistent with relatively high basement permeability, although interpretation of packer tests in Hole 1026B will be complicated by the nonideal hole geometry, because much of the hole below the casing shoe was filled with basalt rubble.

In Hole 1027C, the packer was set first in the casing above open hole. Three slug tests and two injection tests indicate relatively high permeability. The packer was also set outside the casing in Hole 1027C, within the massive basalt flow unit recovered in Core 168-1027C-1R. Two additional slug tests and two injection tests also indicate high permeability. There also appeared to be an underpressure in Hole 1027C, although the magnitude of this underpressure was somewhat lower than that in Hole 1026B. An accurate determination of the natural formation pressure will be made during the long-term CORK experiment.

CORK observatories were set in Holes 1026B and 1027C (Fig. 7). Each observatory included a data logger, pressure gauges above and below the borehole seal, a thermistor string with 10 sensors, and an osmotic sampler above a sinker bar at the bottom of the thermistor cable. Poor drilling conditions in Hole 1026B led to the emplacement of a "liner," a piece of old drill pipe attached to a modified mechanical bit release, that was drilled into the formation and left to hold open the hole. Drilling conditions were considerably better in Hole 1027C, and no liner was required to maintain the hole. Once open holes were established, both CORK systems were emplaced with little difficulty. The first data will be downloaded in about 1 yr during an expedition with the remotely operated vehicle *Jason*.

BURIED BASEMENT TRANSECT
(SITES 1028, 1029, 1030, 1031, and 1032)

Background, Setting, and Goals

In a region spanning 40 to 100 km east of Juan de Fuca Ridge, igneous basement has little relief and is buried by sediments. A suite of parallel seismic lines running perpendicular to the ridge demonstrates that this character is continuous for at least 30 km along strike. Because the sediment layer covering basement is so extensive, this area provides a tempting target for sampling "sealed" basement and for determining accurately the level of total heat loss from young oceanic lithosphere. Local thermal variability was expected to be subdued, particularly because the closest known basement outcrops through which undetected advective heat and chemical exchange could take place are tens of kilometers away.

Accurate determination of the total rate of heat loss from oceanic lithosphere has long been a goal of marine heat-flow surveys. "Calibration" of the theoretical heat flow vs. age relationship would improve estimations of deep-rock properties and of global heat loss using the known distribution of seafloor age and would provide accurate background reference values so that quantitative heat-flow anomalies can be calculated. And, of course, the lithospheric heat-flow budget allows estimation of local and regional hydrothermal budgets. But obtaining high-quality data has been extremely difficult over young crust, because of the perturbing effects of hydrothermal circulation.

Shallow-seafloor heat-flow measurements were attempted across the Buried Basement Transect, but stiff seafloor sediments prohibited probe penetration. Temperature and thermal conductivity data from holes along this part of the overall ODP Leg 168 transect (Sites 1028, 1029, and 1032) were intended to provide accurate estimates of regional basement temperatures. This information, combined with the estimates of depth to basement based on seismic data, was intended to allow calculation of the regional lithospheric heat flux.

Another goal of drilling along the Buried Basement Transect, at shallow basement ridge Sites 1030 and 1031, was to investigate the nature of a high-chloride pore-water anomaly and fluid upflow through the sediments, documented with piston cores in this area. A final goal of operations along the Buried Basement Transect was to obtain a set of "reference" logs through the sediment section. These data would be of interest to Leg 168 scientists, as well as to scientists involved in other regional studies (e.g., Middle Valley, Cascadia Margin).

Scientific Results

The sedimentary succession within the Buried Basement Transect area includes three lithologic units (Fig. 12). Subunit IA is Quaternary in age and is composed of hemipelagic mud (clayey silt to silty clay), thin-bedded turbidites (silt to sandy silt), and thin- to thick-bedded sand turbidites. The base of Subunit IA occurs at approximately 81 mbsf in Hole 1028A and 96 mbsf in Hole 1029A. Sand turbidites are much more common in Hole 1029A. Hole 1028A, conversely, contains more thin-bedded, fine-grained turbidites. The total number of inferred gravity-flow deposits within Subunit IA decreases from 437 at Site 1028 to 388 at Site 1029. Subunit IB is Quaternary in age and is characterized by thin beds of silt and sandy silt intercalated with hemipelagic mud deposits. Erratic increases in the content of calcareous nannofossils generally result in a subtle lightening of color. The top of Subunit IB was not cored at Site 1032. The base of Subunit IB occurs at depths of 107.87 mbsf (Hole 1028A), 197.39 mbsf (Hole 1029A), and 272.47 mbsf (Hole 1032A). The hemipelagic mud deposits of Unit II are Quaternary in age. The thickness of Unit II is 24.6 m in Hole 1028A, 22.7 m in Hole 1029A, and 17.8 m in Hole 1032A. The sediment/basalt contact occurs at curatorial depths of 132.48 and 220.07 mbsf in Holes 1028A and 1029A, respectively. The basement contact is considerably deeper (290.29 mbsf) at Site 1032. Sediments immediately above the basement contact display irregular color variations because of fluctuations in primary clay-mineral content and biogenic carbonate content and/or the hydrothermal formation of clay minerals and Fe-Mn oxides.

We did not subdivide sedimentary deposits from Holes 1030B and 1031A into lithologic units. Each hole contains approximately 41 m of interbedded hemipelagic mud, carbonate-rich mud, and silt to sandy silt turbidites. The hemipelagic deposits at both sites appear to contain unusually high contents of clay-sized material. Although both sites are perched above a prominent basement high, turbidites are significantly more abundant at Hole 1030B. Basalt was recovered only from Hole 1031A. The drillers defined basement contact at approximately 46.9 mbsf in Hole 1030B; the curatorial basement depth in Hole 1031A is 41.30 mbsf. The lowermost deposits at Site 1030 contain abundant nannofossil-rich intervals, but there are no obvious indications of hydrothermal alteration. Basal deposits in Hole 1031A, in contrast, include variegated carbonate-rich claystone, clay-rich siliciclastic mud, and two poorly sorted silt layers with irregular top and bottom contacts and considerable internal disruption. Alteration of these sediments by fluid flow near the basement contact seems likely.

Nannofossils are common to abundant in all Buried Basement sites. They are mostly well preserved, except in Hole 1032A, where they exhibit moderate to strong dissolution. In Hole

1028A, the top of *G. lumina* (130.60 mbsf) and the absence of *Helicosphaera sellii* in the sediment section indicates a basal sediment age younger than 1.55 Ma. In Hole 1029A, the determination of the top of *C. macintyrei* in the basal sediment (220.02 mbsf) suggests an age of 1.58 Ma. The occurrence of *Gephyrocapsa caribbeanica* within the section of Hole 1030B indicates the basal sediment of this hole is younger than 0.76 Ma. In Hole 1031A, the top of *Reticulofenestra asanoi* was recognized at 37.93 mbsf; however, the base of this species (1.15 Ma) was not observed in sediments below that depth. Thus, the age of the basal sediment should be younger than 1.15 Ma. The occurrence of *P. lacunosa* through the section of Hole 1032A suggests that the top of the recovered section (184.52 mbsf) is older than 0.46 Ma, and the absence of *H. sellii* in this section implies the basal sediment is younger than 1.55 Ma. The ages of the basal sediments of these holes are several thousand years younger than basement ages, indicating a hiatus between the formation of basalt and initial sedimentation. Sedimentation rates vary greatly between these holes and show a reduction from the eastern holes to the western holes.

Basement was recovered from Holes 1028A, 1029A, 1031A, and 1032A and consisted predominantly of aphyric, sparsely to moderately phyric, or moderately phyric plagioclase ± olivine ± pyroxene and olivine ± plagioclase basalt. All the rocks recovered are lithologically similar, consisting of pillow basalt. Subunits were identified on the basis of the presence of chilled margins and grain-size changes within the cored sequence, allowing the recognition and logging of individual cooling units. The pillow basalts at Holes 1028A and 1029A are sparsely to moderately phyric, containing 2%-5% plagioclase, 1%-2% olivine, and trace amounts of pyroxene, whereas at Holes 1031A and 1032A, the pillow basalts are aphyric, containing ≤1% to a trace amount of olivine, plagioclase ± pyroxene phenocrysts. All basalts contain ~1%-3% vesicles with diameters ≤1 mm.

Intense secondary alteration affects all rocks recovered from Sites 1028, 1029, 1031, and 1032. Secondary minerals occur as (1) vesicle or cavity linings or fillings; (2) coatings, fracture fillings, and veins; (3) replacement of phenocrysts and microphenocrysts; and (4) patches within mesostasis. The following secondary minerals were identified: clay minerals (saponite and celadonite), iddingsite, calcium carbonate, sulfides, talc, and zeolites. The alteration intensity varies from about 1% to 40% secondary phases. The intensity of glass alteration is relatively high at the Buried Basement sites, particularly at Hole 1032A. Alteration halos, 1-15 mm wide, occur commonly as dark borders on rock pieces or along clay veins.

Haloes are distinguished by the presence of completely filled vesicles, in contrast to empty or saponite-lined and filled vesicles in the gray portion of the rock without halos. The vesicle-filling material is clay, commonly iddingsite and/or celadonite. Hydrothermal veins, typically ≤1 mm wide, include varieties of celadonite, saponite, aragonite, and zeolite minerals.

Alteration temperatures were low, probably less than 100°C, and possibly no higher than the present basement temperatures of 40°-58°C. All of the sites exhibit varying degrees of alteration, including varying degrees of oxidative alteration that required significant open seawater circulation. A subsequent stage characterized by carbonate, saponite, and sulfide alteration may represent relatively closed hydrothermal circulation.

Sediments from Holes 1028A and 1029A exhibit physical properties trends similar to those documented within sediments from the Hydrothermal Transition Transect. The mud-rich layers have lower magnetic susceptibility, thermal conductivity, bulk density, and *P*-wave velocity and higher porosity than the sand-rich layers. Porosity within muddy intervals decreases with depth, following standard compactional trends, whereas *P*-wave velocity increases. There is little difference between the grain density and natural gamma radiation of the mud layers from those of the sand layers. Cores from Holes 1030B and 1031A contain relatively little sand, yet do not appear to show any reduction in porosity with depth. These sediments also have lower magnetic susceptibilities and bulk densities than observed elsewhere along the transect at comparable depths. The physical properties of sediments from Hole 1032A are quite similar to those at the same depths along the Rough Basement Transect.

The concentrations of organic carbon in sediments from the Buried Basement Transect are relatively low and vary broadly within the same range as at the Hydrothermal Transition and Rough Basement Transects. Calculated C/N ratios indicate a predominantly marine origin for organic matter. The hydrocarbon gas content is low and dominated by methane at all sites. Concentrations of methane are significant only where dissolved sulfate is depleted, and concentrations fall to background levels near the seafloor and near basement.

Pore waters from sediments at both Sites 1030 and 1031 provide clear evidence of upward fluid flow. For example, alkalinity normally increases significantly with depth because of organic diagenesis; at Site 1030 it increases slightly before decreasing, and at Site 1031 alkalinity decreases monotonically with depth (Fig. 13). Upward advection seems to be slightly faster at Site 1031 than at Site 1030, as indicated by a contrast between sulfate and ammonia concentrations. It appears that there is a balance between the input of ammonia by bacterial breakdown of organic matter and the rate at which pore-water advection removes ammonia from the sediment pores. Chloride concentrations increase with depth, approaching or slightly exceeding values believed to have been present in Pleistocene glacial seawater. Concentrations remain elevated at depth and are associated with low Mg, K, and Si concentrations. The elevated chloride values are significantly greater than any others seen during Leg 168. The fluid moving upward from basement over the ridge at Sites 1030 and 1031 is geochemically more mature than the fluid found at adjacent sites, showing effects of extensive hydration reactions. These observations may indicate a deeper reaction zone and/or a longer residence time in basement.

Sites 1028, 1029, and 1032 form a west-to-east transect east of the buried ridge where Sites 1030 and 1031 were drilled. The pore waters from these sites show features typical of organic diagenesis (e.g., rapid decrease in sulfate and increase in alkalinity, ammonia, and phosphate with depth) and inferred mineral reactivity (calcium and magnesium minima) seen elsewhere, as well as evidence for partially evolved seawater in basement (as is apparent from the increase in sulfate and calcium and decrease in alkalinity with depth).

There are complications to this simple picture. Sulfate in near-basement pore waters is low at Site 1028 and forms a natural extension to the sequence seen at the Hydrothermal Transition sites (Fig. 14) (apart from the Sites 1030 and 1031 data). However, near-basement sulfate is higher at Site 1029 than at Site 1028 and this seems to be a break in the overall geochemical pattern. In contrast, calcium increases systematically, and values near basement at Site 1032 are considerably greater than those measured at a nearby basement outcrop. This observation most likely indicates that there is a reaction zone where Ca and Na are exchanged very close to the sediment/basement interface.

Sediment temperatures were measured at all sites along the Buried Basement transect. Along a transect from west to east, Sites 1030/31, 1028, 1029, and 1032 have extrapolated temperatures at the sediment/basement contact of approximately 40°, 51°, 59°, and 57°C, respectively. The 40°C basement temperature at shallow-ridge Sites 1030 and 1031 correspond to heat flow close to 1 W/m^2. These high heat-flow values are consistent with the ridge being a fluid upflow zone, as indicated by the inorganic pore-water data. The remaining basement temperatures are considerably lower than would be expected if the crust was indeed fully sealed from exchange of hydrothermal fluids with the overlying ocean. In fact, upper basement temperatures at Sites 1029 and 1032 are remarkably close to the upper basement temperature of 61°-64°C at Rough Basement Sites 1026 and 1027, about 28 km east of Site 1032. Because of uncertainties in the actual location of the most hydrothermally active part of upper basement, these similar temperature values may indicate relative thermal homogeneity over a remarkable distance of nearly 50 km. If fluid flow actually occurs on such a crustal scale, this will require a substantial revision of many conceptual models of heat and mass transfer in the upper oceanic crust.

Logging was completed in Hole 1032A during the last days of scientific operations. Although the hole was drilled well into basement with the hope of obtaining high-quality measurements across the sediment/basement contact, hole fill and bridging problems prevented passage of the tools to this depth. Three tool strings (triple-combination, Formation MicroScanner [FMS]/sonic, and geochemical) were run successfully over the upper 275-280 m of sediment in the hole.

SUMMARY AND PRINCIPLE CONCLUSIONS

The primary scientific objectives of Leg 168, as outlined in the Scientific Prospectus, were to

1. *determine the thermophysical characteristics of hydrothermal circulation in the upper oceanic crust in off-axis settings as influenced by crustal topography, sediment cover, and permeability;*
2. *determine the sensitivity of crustal fluid composition to the age, temperature, and degree of sediment burial of the igneous crust;*
3. *examine the nature and fundamental causes of physical consolidation and mineralogical and chemical alteration of the igneous crust as functions of age and degree of sediment burial; and*
4. *improve constraints on the fluxes of heat and elements between the permeable igneous crust*

and the overlying ocean.

In the following preliminary summary of results, individual interpretations are related to the above objectives where appropriate.

Leg 168 drilling sites were placed along a transect on the eastern flank of the Juan de Fuca Ridge, extending from about 20 km east of the ridge crest, where turbidite sediments begin to continuously blanket the 0.8-Ma igneous crust, to about 100 km from the crest, where the crust is 3.6 Ma in age. Coring and downhole measurements completed along this transect have provided unprecedented documentation of the efficiency with which water transports heat and solutes laterally in the upper oceanic crust and of the consequences of that circulation (Objectives 1, 2, 3, and 4). Additional information from long-term hydrologic observatories (CORKs) established at four of the sites will provide valuable quantitative constraints on the pressures that drive fluid flow, on basement-water composition, and on the details of the thermal structure in the uppermost oceanic crust as it is influenced by hydrothermal circulation (Objectives 1, 2, and 4).

A simple sedimentation history is inferred at each of the sites, with locally carbonate-enriched hemipelagic deposition beginning to accumulate some thousands of years after creation of the igneous crust, followed at the older sites by periods of accumulation of hemipelagic muds and fine turbidites, and finally by a Pleistocene sequence of variably thick silt- and sand-turbidites interbedded with hemipelagic muds. Despite the frequency of sandy layers in the upper part of the sections, this blanket of sediment that buries all primary topography of the igneous crust by up to 600 m is generally impermeable and prevents fluid flow at geochemically significant rates except where the section thins to less than about 100 m over local basement highs (Objective 2). At three such sites (Sites 1025, 1030, and 1031) there is clear evidence in the pore-fluid compositional profiles of discharge, although the seepage velocity is far too low to be thermally significant. The integrated effect of fluid seepage in the form of sediment alteration is virtually undetectable; at all sites, sediment alteration was evident only on a scale of up to a few meters above the basement contact (Objective 3).

Basalts were recovered at nearly all sites, and they represent a wide range of compositions and textures: normal tholeiitic pillows; massive, highly fractionated flows with extremely large (up to 1 cm) vesicles; volcanic breccias cemented with low-temperature hydrothermal mineralization; and a massive diabase unit erupted onto or intruded into the sediment section well off-axis. Alteration of the igneous rock varies in intensity from site to site along the transect, both as a consequence of increasing temperature and increasing degree of basement-water isolation and as a result of variations in texture and lithology (Objectives 1 and 3). Fresh olivines present at Site 1023 indicate that these aphanitic samples—the youngest, coolest, and closest to a source of fresh seawater (about 3 km from the nearby region of outcropping basement)—have undergone the least amount of alteration. In contrast, practically all olivines in the massive, coarser-grained units at Site 1025 are completely replaced by a mixture of clay minerals (primarily saponite with some celadonite), minor carbonate, and rare talc and chlorite/smectite. Samples from sites throughout the transect contain mineral linings or complete mineral fillings of vesicles. At the oldest and hottest Sites 1026 and 1027, the vesicle filling involves two to four sequential layers. The observed distribution of the various vesicle fills is systematic, in detail linked to the proximity of the vesicles to veins and alteration haloes. Rocks at nearly all sites (except from the massive units) exhibit varying degrees of oxidative alteration that required significant open-seawater circulation. A subsequent stage characterized by carbonate, saponite, and sulfide alteration probably represents relatively closed hydrothermal circulation following sediment burial. No alteration, including that represented by vein-filling minerals, was observed that requires temperatures much higher than those prevailing today (Objective 3).

Active and highly efficient local advective heat and chemical transport is evident in the degree of homogenization of crustal fluid temperatures and compositions (Objectives 1 and 3). Sites 1026 and 1027, drilled ~2.2 km apart into a sediment-buried basement ridge and adjacent trough, respectively, encountered basement at virtually identical temperatures (~64°C), despite the large contrast in the thickness of sediment at the ridge and valley sites, 250 and 600 m, respectively (Objective 2). Basement-fluid compositions, inferred from pore waters squeezed from near-basal sediments and sampled directly from the discharging Site 1026, are also to a first order identical at the two sites, and identical to water sampled at a seafloor vent roughly 7 km away where water discharges through the seafloor at an isolated, small basement outcrop.

Some form of regional-scale flow is also inferred on the basis of thermal and geochemical observations made across the full length of the transect (Objectives 1, 2, and 4). A comparison of seafloor heat-flow measurements with the total expected from the cooling lithosphere beneath shows a clear deficit on this sediment-sealed eastern ridge flank out to a distance of at least 20-30 km from the nearest basement outcrop; it has been inferred that this deficit reflects the heat lost advectively from the upper igneous crust through regions of outcropping basement through lateral fluid flow. Observations at the first three sites of the Leg 168 transect substantiate this inference. Clear gradients in basement temperature and basement-water chemistry were documented, with temperatures at the sediment/basement contact increasing systematically with distance from the region of outcropping basement, from approximately 15°C at Hole 1023A, to 22°C at Site 1024, and to 38°C at Site 1025 (Objectives 1, 3, and 4). This trend is opposite to that expected, given the increasing age and decreasing sediment thickness across this part of the drilling transect; it is best explained by rapid fluid flow and heat transport in the upper basement rocks beneath the sediment section, with cool seawater recharge supplied in the area of extensive igneous outcrop near the ridge crest. Basement-water compositions revealed systematic changes with increasing temperature and distance from the outcrop in many elemental concentrations, including magnesium and calcium, which are particularly reactive in basement. Elemental concentrations at Site 1023, situated 3.5 km away from the line of abrupt basement outcrop to the west, were changed only slightly from seawater, whereas water at Site 1025, nearly 16 km away, showed significant reaction with basement (Objective 2). Basement-water chlorinity values also showed clear signs of lateral flow in basement, with the influence of post-Pleistocene seawater, only a few thousand years old, seen beneath the sediment cover also as far away from the basement outcrop as Site 1025.

Perhaps the most remarkable conclusion from the results of the leg concerns the scale over which significant lateral heat and chemical transport must take place (Objectives 1 and 4). Over most of the length of the transect the local average heat flow through the sediment section does not exceed about 80% of the amount expected from the lithosphere beneath. Basement temperatures simply continue to increase systematically with distance from the region of basement outcrop near the ridge to the maximum temperature at Sites 1026 and 1027 noted previously. This disagreement with lithospheric cooling theory may point to a fundamental lack of understanding of lithospheric heat loss, but it is more likely that a significant quantity of heat is lost advectively from beneath the sediment seal over distances of many tens of kilometers. This conclusion is supported by the level of sulfate observed in basement waters, which falls systematically with distance from the region of basement outcrop but to a remarkably elevated minimum of 18 mmol/kg at the most distant Sites 1026 and 1027 (Objectives 3 and 4). At all sites, the sediment section is seen to serve as a very efficient sink of sulfate; the only source for replenishment is seawater supplied via purely-basement pathways. Very large distances of lateral transport (up to 80 km) are implied.

The primary scientific objectives of this phase of ridge-flank drilling focused on lateral thermal and chemical gradients associated with hydrothermal circulation, and they were achieved with highly limited basement penetration. Virtually all observations can probably be accounted for with a hydrothermal system that is dominated by fluid flow in only the upper tens to few hundreds of meters of the igneous oceanic crust. However, some hints of deeper levels of fluid flow are suggested at Sites 1030/31, which penetrated a basement ridge where anomalous basement fluids appear to be present (Objectives 1, 2, and 4). Chlorinity and the concentrations of Mg and Ca in basement water are anomalous with respect to the trends defined by other sites of the transect and suggest reactions at a temperature much higher than that at the top of the crust; basement fluids here may be "contaminated" by water flow locally up a fault zone from a depth where temperatures and fluid residence times are greater.

Although ODP Leg 168 was highly successful in setting strong constraints on the rates of fluid flow through the uppermost igneous crust and in beginning to identify the surprisingly large lateral scale over which hydrothermal circulation can operate, the need for additional work in this area is clear. Determining the routes of flow, including the hydrologic role of normal faults and the depth of penetration of significant circulation, will require deeper sampling and downhole experiments possible only through a second leg of drilling. Effort must also be given to better identifying the locations and details of seawater recharge and crustal water discharge, where very large chemical and heat fluxes must occur.

FIGURE CAPTIONS

Figure 1. Location map.

Figure 2. Magnetic anomaly map of the crust modified from the Leg 168 Scientific Prospectus. Sites were located by gridding between half-minute marks.

Figure 3. Leg 168 sites and Hydrocell 95 seismic lines.

Figure 4. Stratigraphic summary for the HT Transect area. Bed thicknesses are schematic. D = drilling depth, R = recovery depth, and L = lithology. Sediment composition is indicated by the white (turbidite sands), black (silts), and dark gray (muds) colors.

Figure 5. Composition of pore waters from Hydrothermal Transition sites. The arrows denote the composition of bottom seawater. Sample locations are denoted by solid circles (Hole 1023A), open circles (Holes 1024A and 1024B), and solid triangles (Holes 1025A and 1025B).

Figure 6. Comparison of Hydrothermal Transition seafloor (circles) and three borehole (squares) heat-flow determinations illustrates a good match between the two data sets.

Figure 7. Configurations of the downhole sensor strings deployed in the CORK experiments in HT Transect Holes 1024C and 1025C, and RB Transect Holes 1026B and 1027C.

Figure 8. Stratigraphic summary for the Rough Basement Transect area. Bed thicknesses are not shown to scale. Sediment composition is indicated by the white (turbidite sands), black (silts), and dark gray (muds) colors.

Figure 9. Summary of the rock types, lithological units and range of phenocrysts and groundmass minerals present at Holes 1026B, 1026C, 1027B, and 1027C, listing the diagnostic petrological features of each unit. The soft, firm, and hard pattern boxes represent the driller's estimate of the ease of drilling. VCD = Visual Core Description sheets, D = drilling depth, R = recovery depth, and L = lithology.

Figure 10. Composition of pore waters from Rough Basement sites. Arrows denote the composition of bottom seawater. Sample locations are denoted by solid circles (Holes 1026A and 1026C), solid diamonds (1026 WSTP; plotted at the depth in basement where these waters originated before flowing into the cased hole), open circles (Holes 1027B and 1027C) and open diamonds (Baby Bare springs; G. Wheat and M. Mottl, unpublished data; plotted below the sediment section for comparison.

Figure 11. A. Comparison of Rough Basement Transect seafloor (circles) and three borehole (squares) heat-flow determinations. **B.** Open-hole temperatures versus depth recorded with the DVTP and APC tool 11 (two deployments) in Hole 1026B. The tools were held at the depths shown for several minutes to allow thermal equilibration.

Figure 12. Stratigraphic summary for the BB Transect area. Bed thicknesses are not shown to scale. Sediment composition is indicated by the white (turbidite sands), black (silts), and dark gray (muds) colors.

Figure 13. Composition of pore waters from Buried Basement sites. The arrows denote the composition of bottom seawater. Sample locations are denoted by solid circles (Site 1030) and open circles (Site 1031).

Figure 14. Composition of pore waters from Buried Basement sites. The arrows denote the composition of bottom seawater. Sample locations are denoted by solid circles (Site 1028), open circles (Site 1029), and solid triangles (Site 1032).

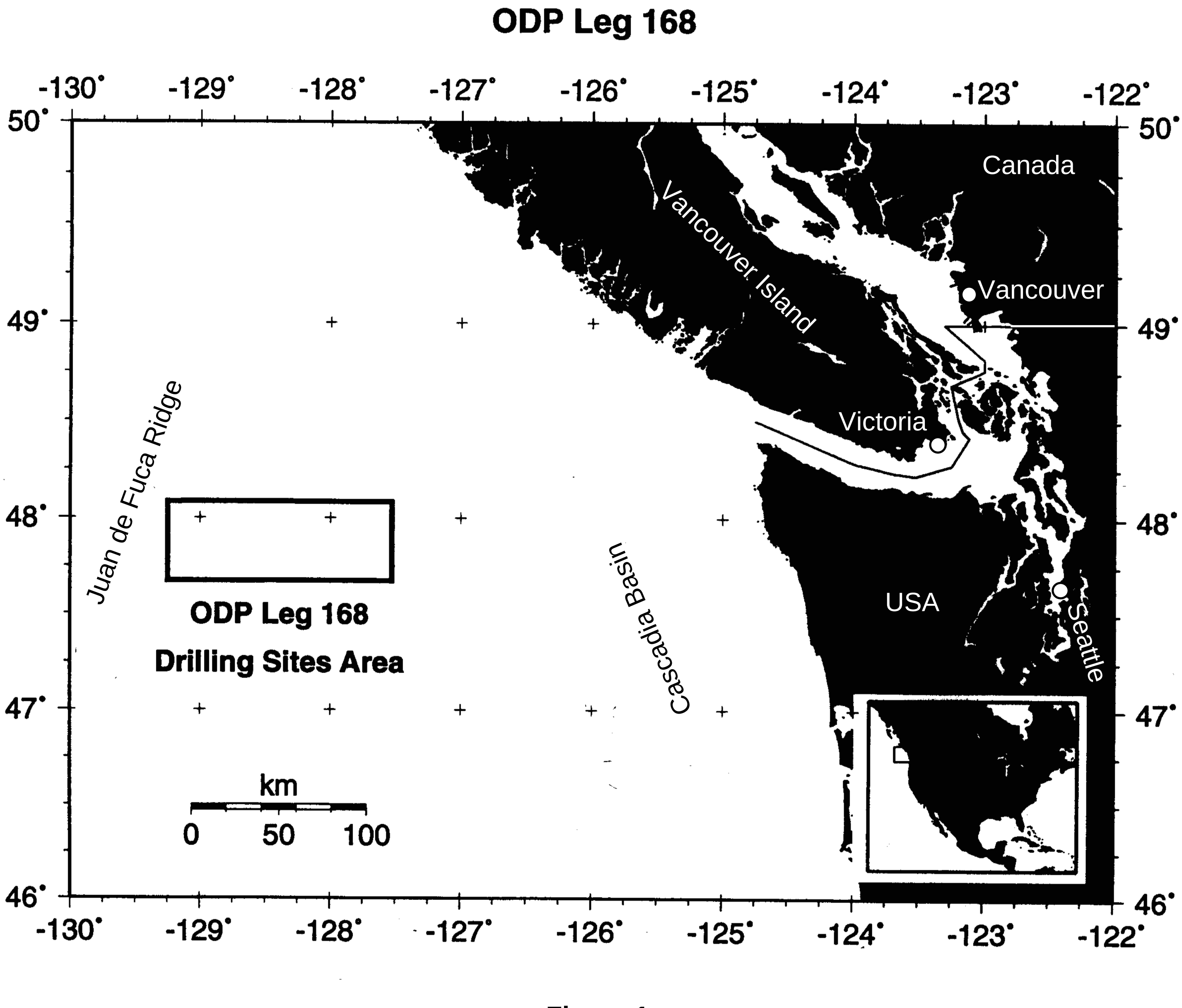
ODP Leg 168
-130° -129° -128° -127° -126° -125° -124° -123° -122°
50° 49° 48° 47° 46°
Canada
Vancouver Island
Vancouver
Victoria
Juan de Fuca Ridge
ODP Leg 168
Drilling Sites Area
Cascadia Basin
USA
Seattle
km
0 50 100

Figure 1

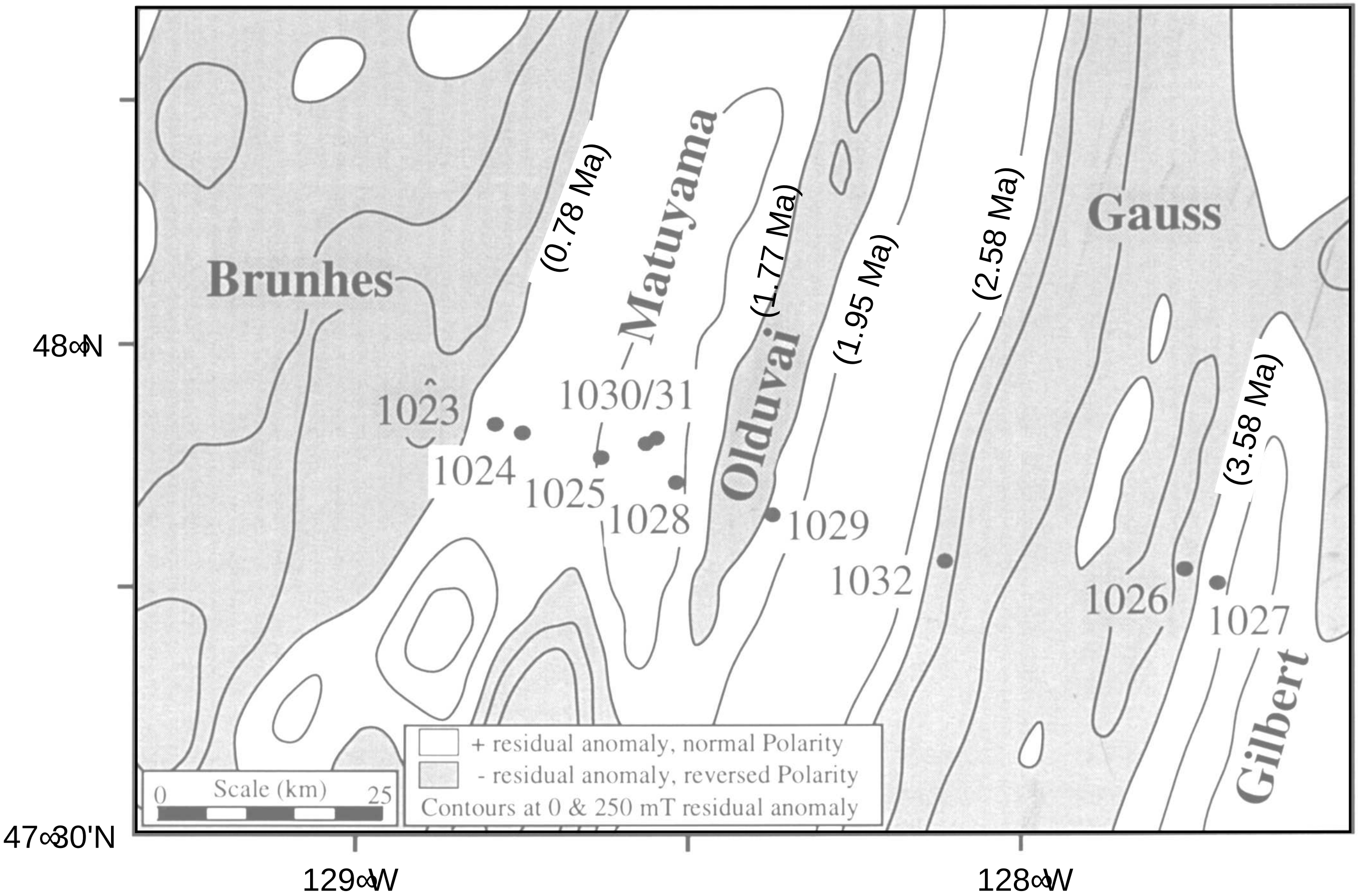

48∞N
47∞30'N
129∞W
128∞W
Brunhes
Matuyama
Olduvai
Gauss
Gilbert
(0.78 Ma)
(1.77 Ma)
(1.95 Ma)
(2.58 Ma)
(3.58 Ma)
1023
1024
1025
1028
1030/31
1029
1032
1026
1027
+ residual anomaly, normal Polarity
- residual anomaly, reversed Polarity
Contours at 0 & 250 mT residual anomaly
Scale (km)
0
25

Figure 2

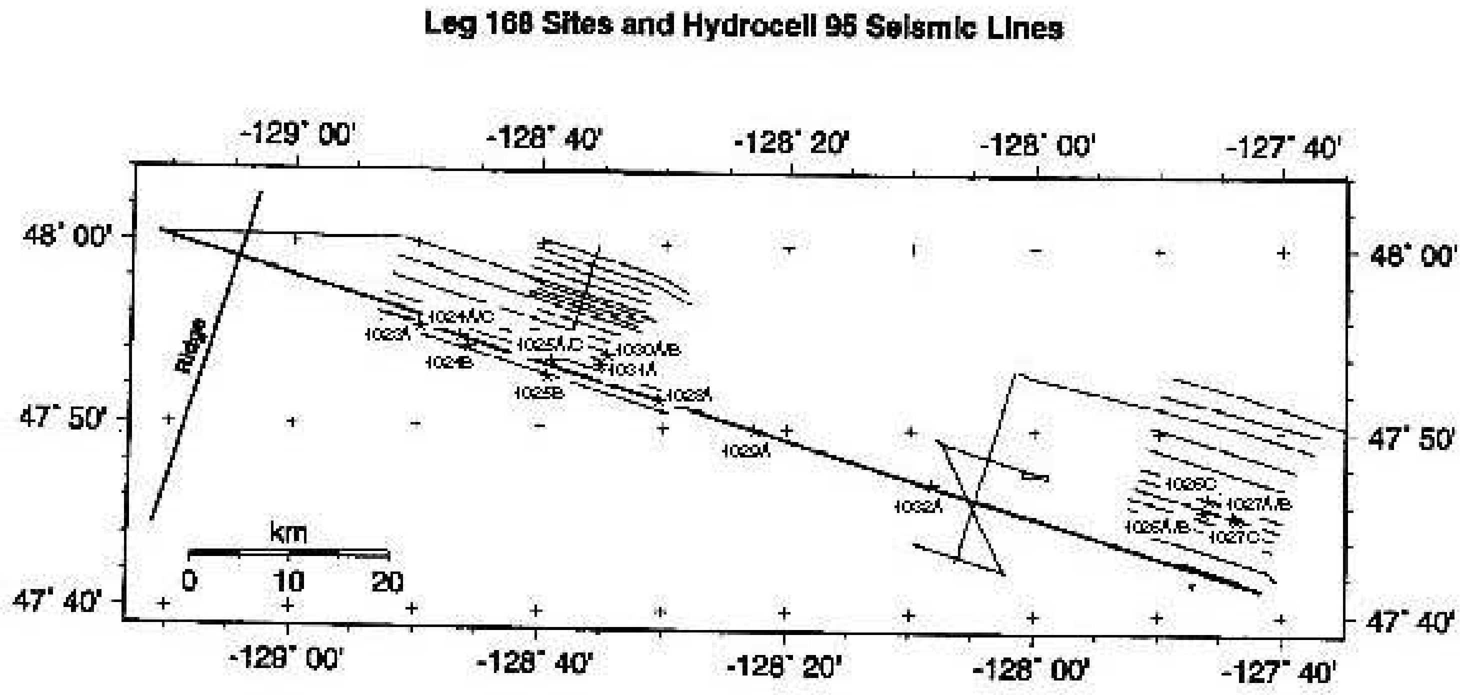
Leg 168 Sites and Hydrocell 95 Seismic Lines
-129° 00'
-128° 40'
-128° 20'
-128° 00'
-127° 40'
48° 00'
47° 50'
47° 40'
Ridge
km
0
10
20
1023A
1024A/C
1024B
1025A/C
1025B
1030A/B
1031A
1028A
1029A
1032A
1026C
1027A/B
1026A/B
1027C

Figure 3

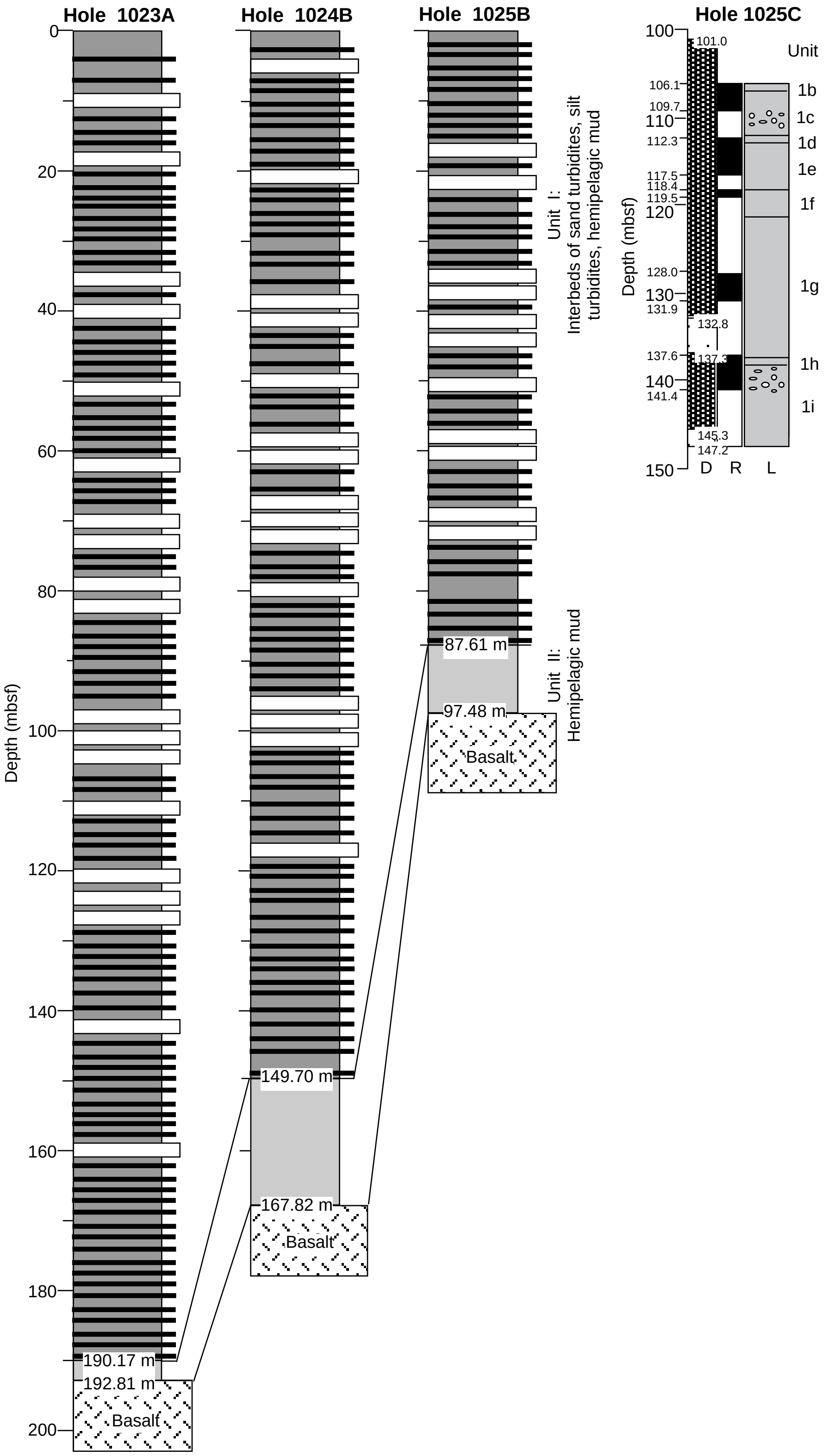

Hole 1023A
Hole 1024B
Hole 1025B
Hole 1025C
Depth (mbsf)
0
20
40
60
80
100
120
140
160
180
200
190.17 m
192.81 m
Basalt
149.70 m
167.82 m
Basalt
87.61 m
97.48 m
Basalt
Unit I: Interbeds of sand turbidites, silt turbidites, hemipelagic mud
Unit II: Hemipelagic mud
100
110
120
130
140
150
101.0
106.1
109.7
112.3
117.5
118.4
119.5
128.0
131.9
132.8
137.6
137.3
141.4
145.3
147.2
D
R
L
Unit
1b
1c
1d
1e
1f
1g
1h
1i

Figure 4

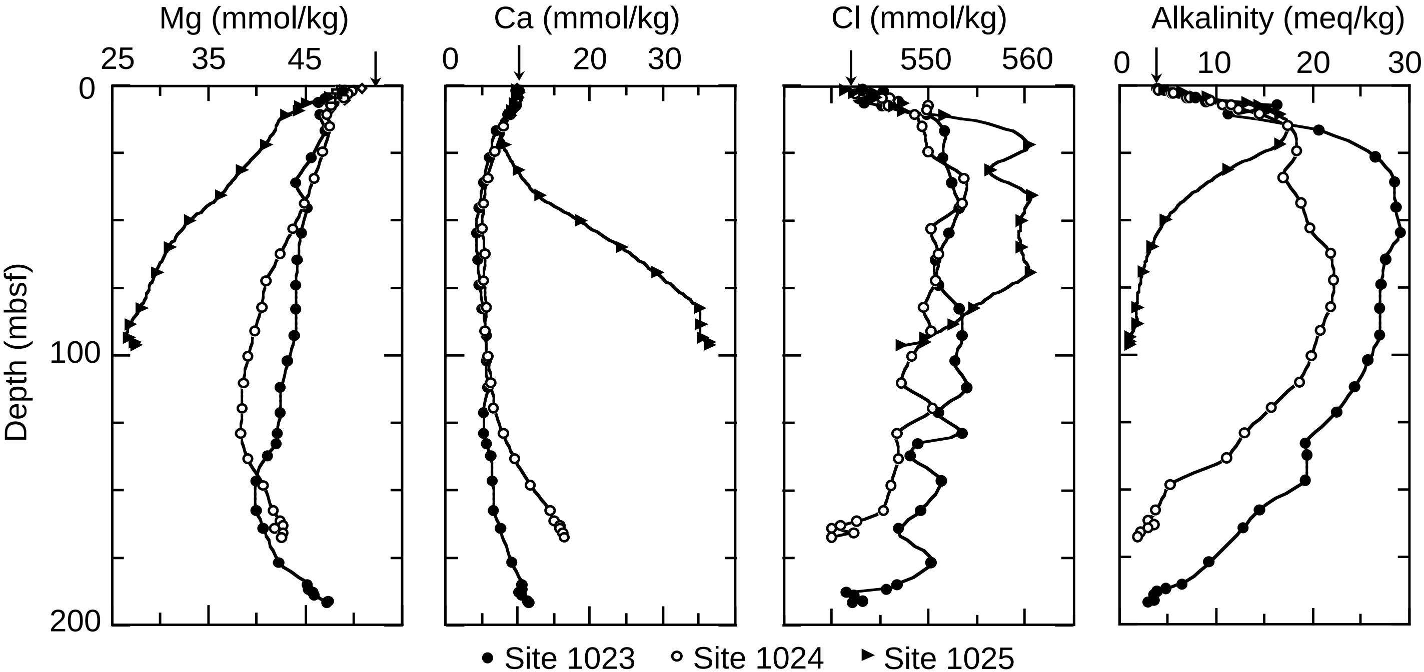

Mg (mmol/kg)
25
35
45
Ca (mmol/kg)
0
20
30
Cl (mmol/kg)
550
560
Alkalinity (meq/kg)
0
10
20
30
0
100
200
Depth (mbsf)
Site 1023
Site 1024
Site 1025

Figure 5

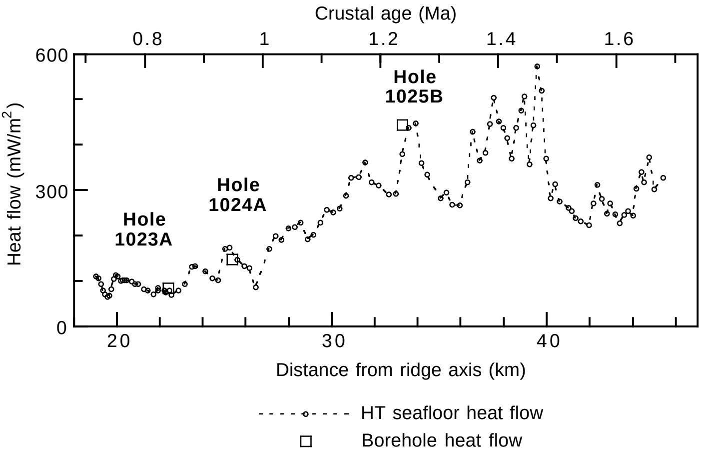
Crustal age (Ma)
0.8
1
1.2
1.4
1.6
600
300
0
Heat flow (mW/m2)
Hole 1023A
Hole 1024A
Hole 1025B
20
30
40
Distance from ridge axis (km)
HT seafloor heat flow
Borehole heat flow

Figure 6

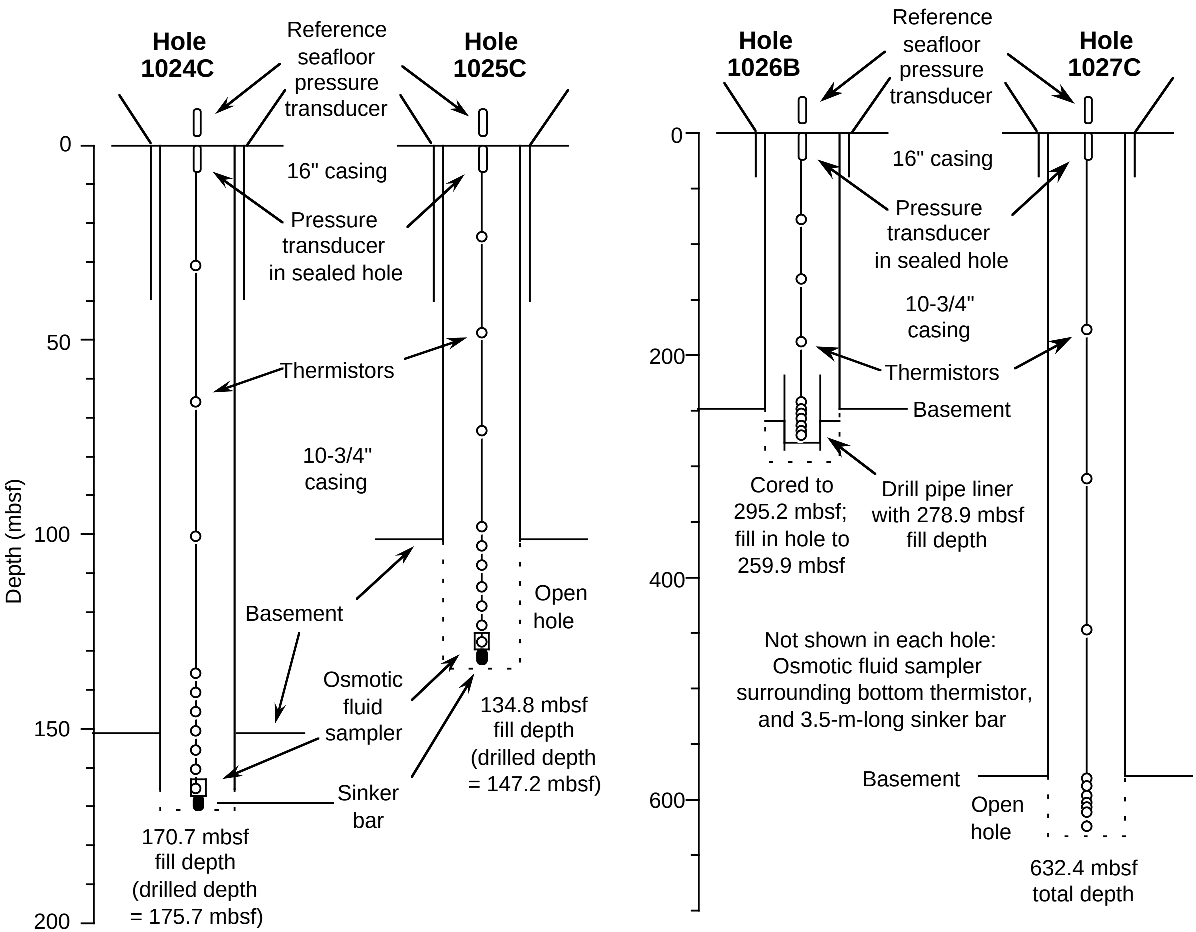

Hole 1024C
Hole 1025C
Hole 1026B
Hole 1027C
Reference seafloor pressure transducer
16" casing
Pressure transducer in sealed hole
10-3/4" casing
Thermistors
Basement
Osmotic fluid sampler
Sinker bar
Open hole
170.7 mbsf fill depth (drilled depth = 175.7 mbsf)
134.8 mbsf fill depth (drilled depth = 147.2 mbsf)
Cored to 295.2 mbsf; fill in hole to 259.9 mbsf
Drill pipe liner with 278.9 mbsf fill depth
Not shown in each hole: Osmotic fluid sampler surrounding bottom thermistor, and 3.5-m-long sinker bar
632.4 mbsf total depth
Depth (mbsf)
0
50
100
150
200
0
200
400
600

Figure 7

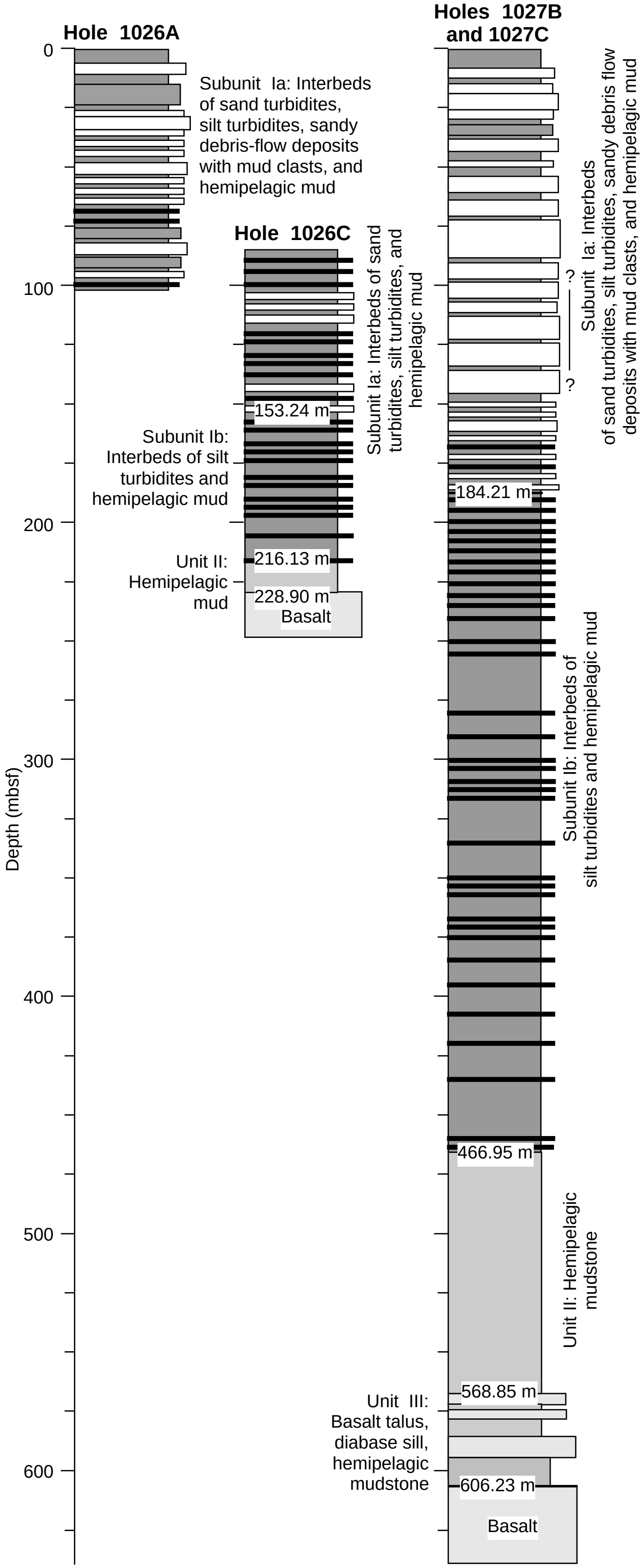

Hole 1026A
Holes 1027B and 1027C
Hole 1026C
0
100
200
300
400
500
600
Depth (mbsf)
Subunit Ia: Interbeds of sand turbidites, silt turbidites, sandy debris-flow deposits with mud clasts, and hemipelagic mud
Subunit Ia: Interbeds of sand turbidites, silt turbidites, and hemipelagic mud
153.24 m
Subunit Ib: Interbeds of silt turbidites and hemipelagic mud
216.13 m
Unit II: Hemipelagic mud
228.90 m
Basalt
Subunit Ia: Interbeds of sand turbidites, silt turbidites, sandy debris flow deposits with mud clasts, and hemipelagic mud
?
?
184.21 m
Subunit Ib: Interbeds of silt turbidites and hemipelagic mud
466.95 m
Unit II: Hemipelagic mudstone
568.85 m
Unit III: Basalt talus, diabase sill, hemipelagic mudstone
606.23 m
Basalt

Figure 8

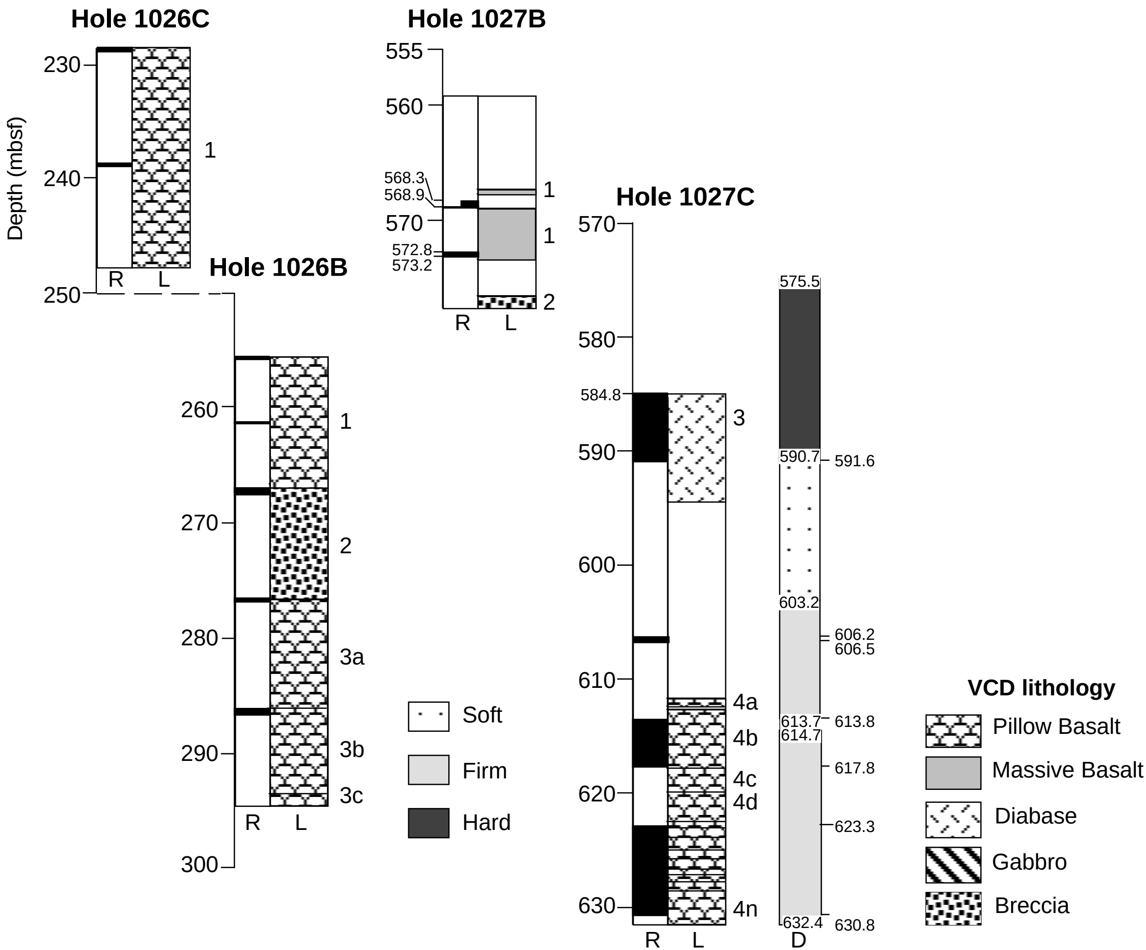
Hole 1026C
Depth (mbsf)
230
240
250
R
L
1
Hole 1026B
260
270
280
290
300
1
2
3a
3b
3c
R
L
Hole 1027B
555
560
568.3
568.9
570
572.8
573.2
1
1
2
R
L
Soft
Firm
Hard
Hole 1027C
570
580
584.8
590
600
610
620
630
3
4a
4b
4c
4d
4n
R
L
575.5
590.7
591.6
603.2
606.2
606.5
613.7
613.8
614.7
617.8
623.3
632.4
630.8
D
VCD lithology
Pillow Basalt
Massive Basalt
Diabase
Gabbro
Breccia

Figure 9

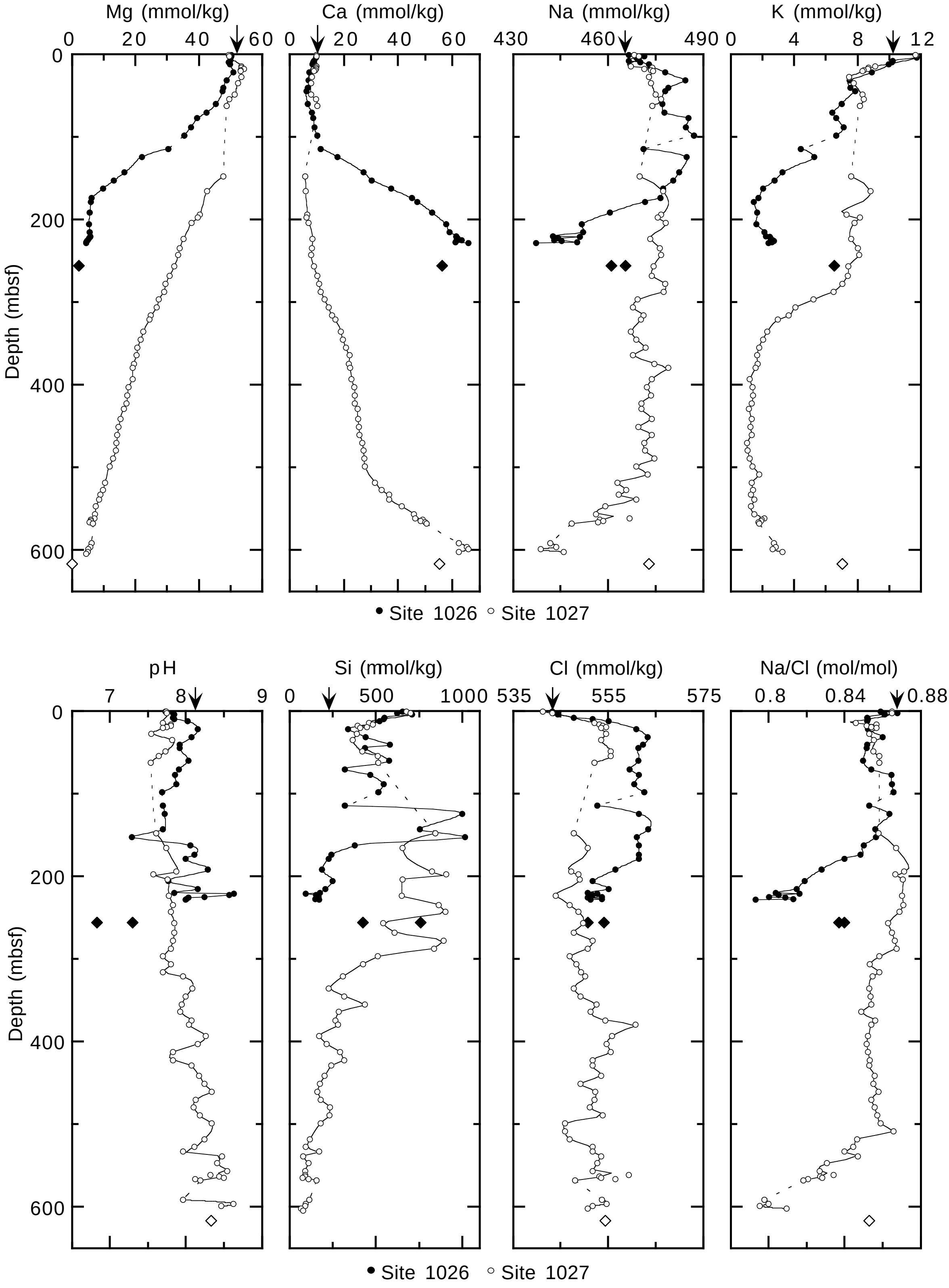
Mg (mmol/kg)
0
20
40
60
Ca (mmol/kg)
0
20
40
60
Na (mmol/kg)
430
460
490
K (mmol/kg)
0
4
8
12
Depth (mbsf)
0
200
400
600
Site 1026
Site 1027
pH
7
8
9
Si (mmol/kg)
0
500
1000
Cl (mmol/kg)
535
555
575
Na/Cl (mol/mol)
0.8
0.84
0.88
Depth (mbsf)
0
200
400
600
Site 1026
Site 1027

Figure 10

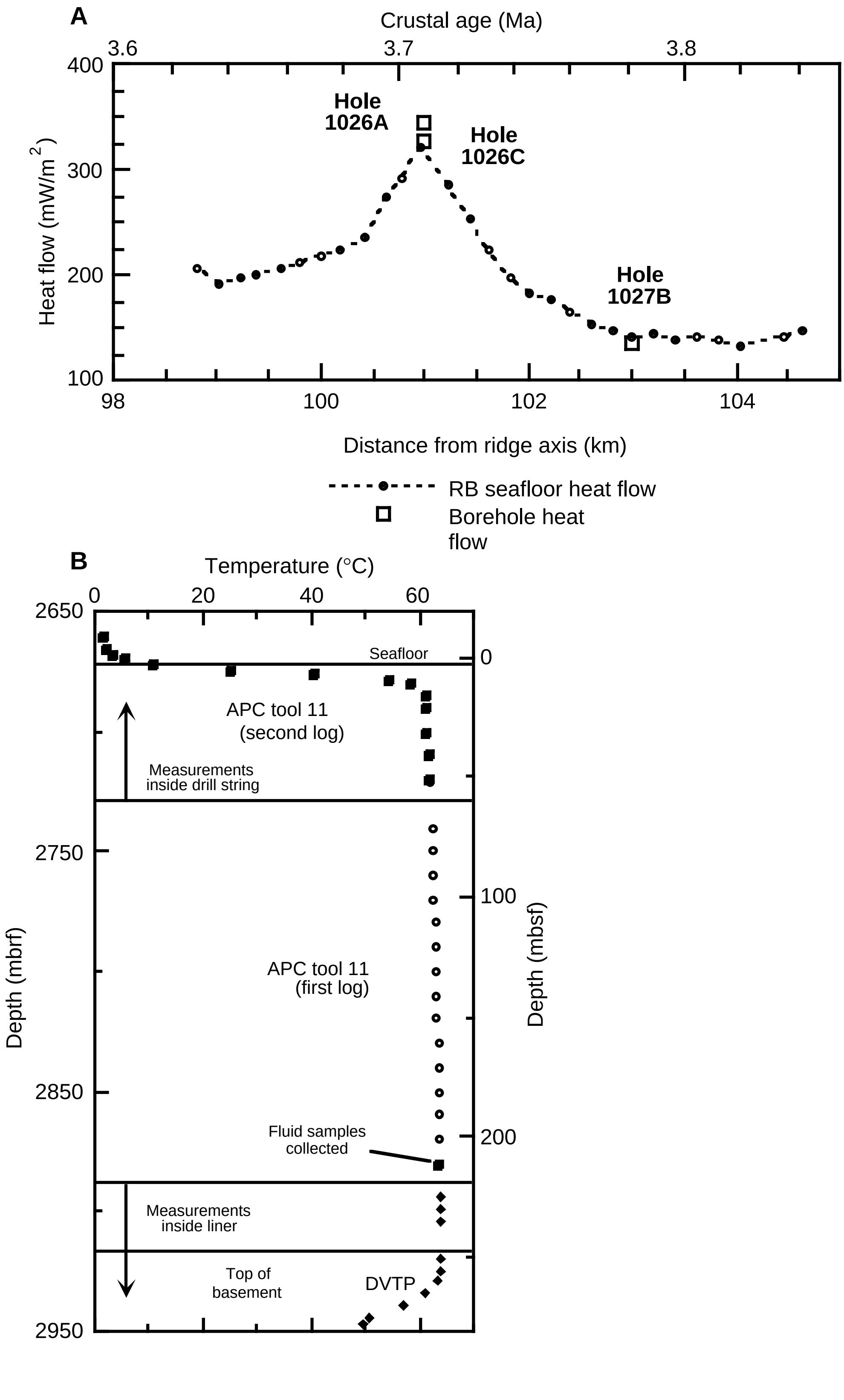
A
Crustal age (Ma)
3.6
3.7
3.8
400
300
200
100
Heat flow (mW/m 2)
Hole 1026A
Hole 1026C
Hole 1027B
98
100
102
104
Distance from ridge axis (km)
RB seafloor heat flow
Borehole heat flow
B
Temperature (°C)
0
20
40
60
2650
2750
2850
2950
Depth (mbrf)
0
100
200
Depth (mbsf)
Seafloor
APC tool 11 (second log)
Measurements inside drill string
APC tool 11 (first log)
Fluid samples collected
Measurements inside liner
Top of basement
DVTP

Figure 11

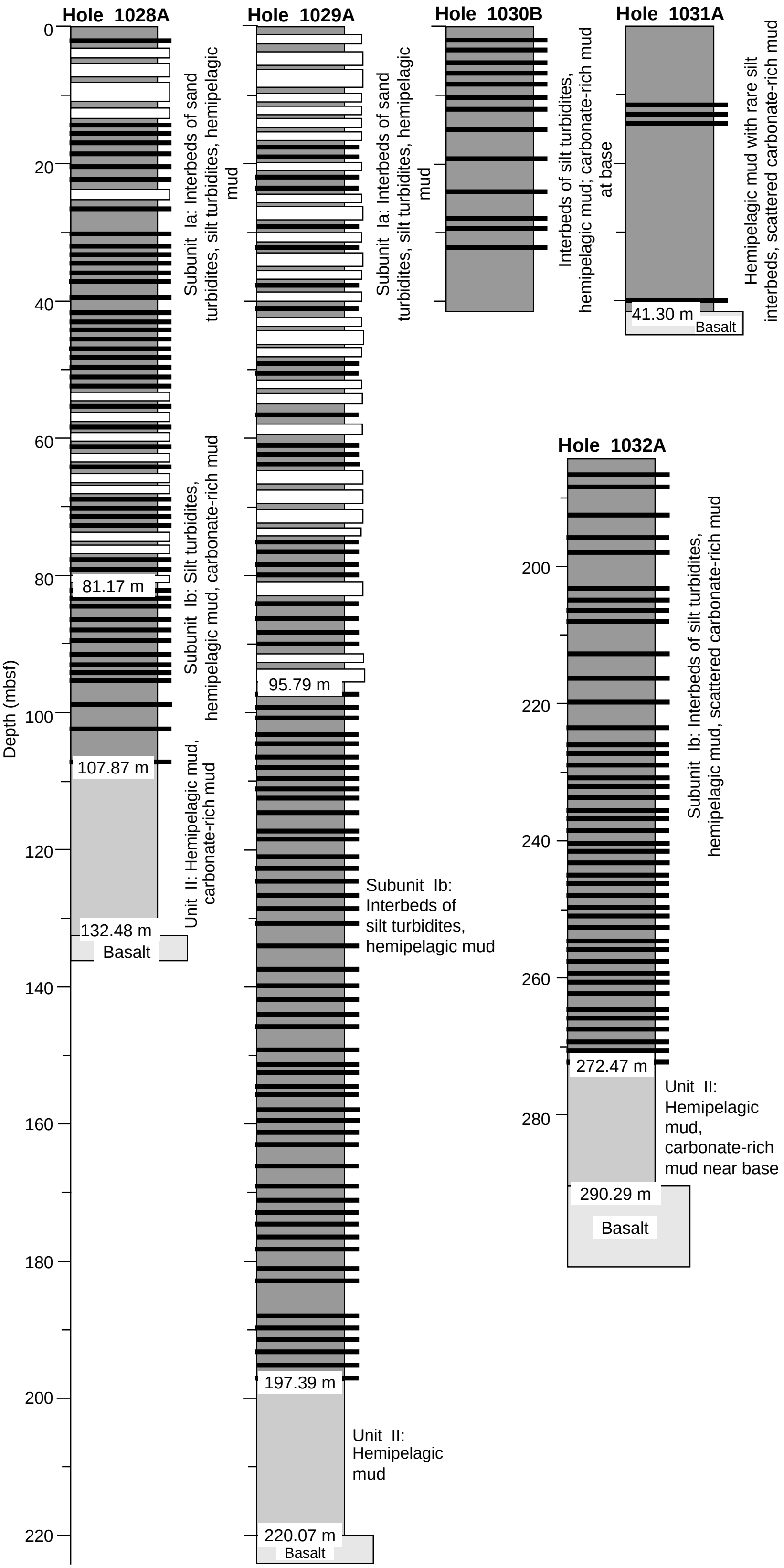
Hole 1028A
Hole 1029A
Hole 1030B
Hole 1031A
Hole 1032A
Depth (mbsf)
0
20
40
60
80
100
120
140
160
180
200
220
240
260
280
Subunit Ia: Interbeds of sand turbidites, silt turbidites, hemipelagic mud
Subunit Ib: Silt turbidites, hemipelagic mud, carbonate-rich mud
Unit II: Hemipelagic mud, carbonate-rich mud
81.17 m
107.87 m
132.48 m
Basalt
95.79 m
Subunit Ib: Interbeds of silt turbidites, hemipelagic mud
197.39 m
Unit II: Hemipelagic mud
220.07 m
Interbeds of silt turbidites, hemipelagic mud; carbonate-rich mud at base
Hemipelagic mud with rare silt interbeds, scattered carbonate-rich mud
41.30 m
Subunit Ib: Interbeds of silt turbidites, hemipelagic mud, scattered carbonate-rich mud
272.47 m
Unit II: Hemipelagic mud, carbonate-rich mud near base
290.29 m

Figure 12

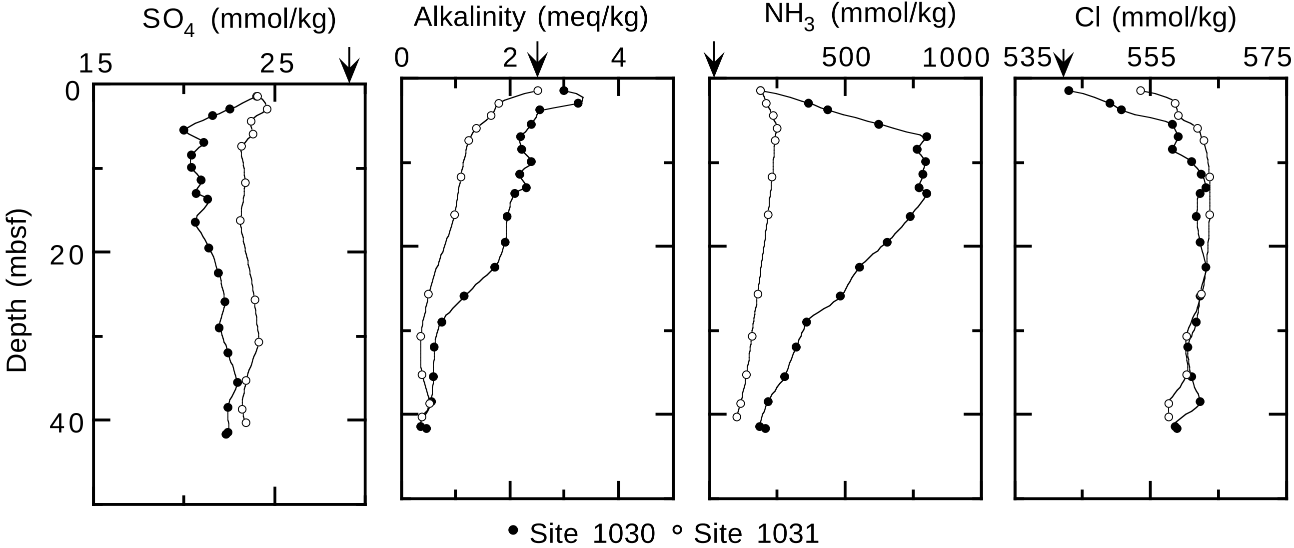

SO4 (mmol/kg)
15
25
Alkalinity (meq/kg)
0
2
4
NH3 (mmol/kg)
500
1000
Cl (mmol/kg)
535
555
575
0
20
40
Depth (mbsf)
• Site 1030 ∘ Site 1031

Figure 13

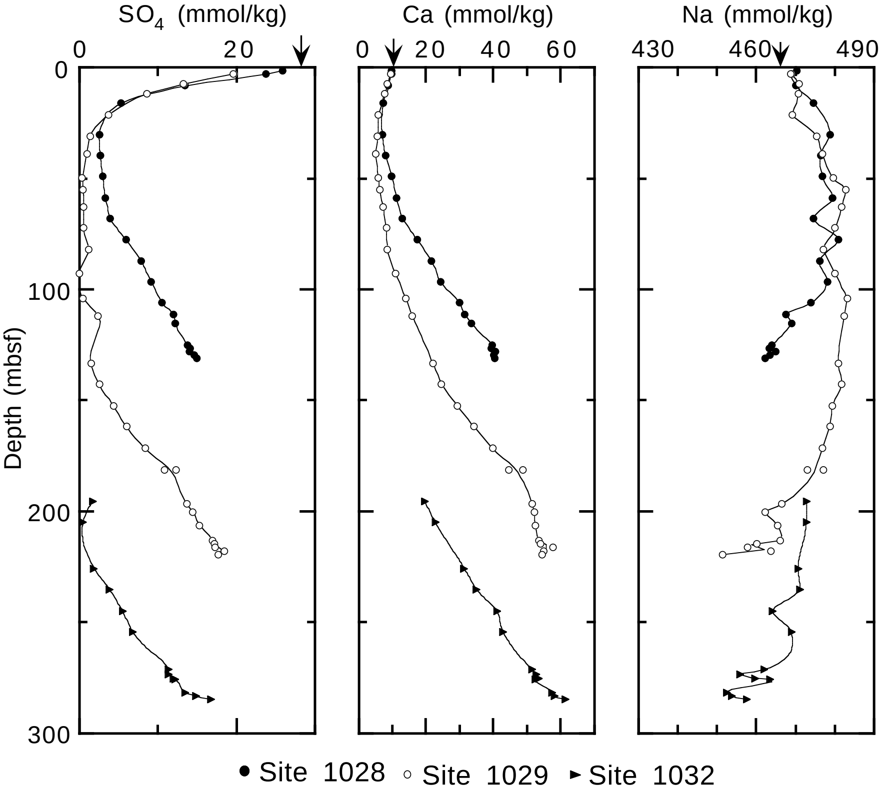
SO4 (mmol/kg)
Ca (mmol/kg)
Na (mmol/kg)
0
20
0
20
40
60
430
460
490
0
100
200
300
Depth (mbsf)
Site 1028
Site 1029
Site 1032

Figure 14

OPERATIONS SYNOPSIS

The ODP Operations and Engineering personnel aboard *JOIDES Resolution* for Leg 168 were:

Operations Manager:	Michael Storms
Schlumberger Engineer:	Steve Kittredge
ODP Development Engineer:	Bill Rhinehart

SITE 1023
(Proposed Site HT-2A)

Hole 1023A

The ship left San Francisco at roughly 9:00 a.m., 20 September, 1996. Fresh northerly headwinds were encountered while sailing to Site 1023, which slowed the vessel's speed occasionally to less than 9 kt. Conditions continued to moderate throughout the transit, and speeds improved to 11.0 kt on the final day. A standard advanced hydraulic piston core/extended core barrel (APC/XCB) bottom-hole assembly (BHA) was deployed without a nonmagnetic drill collar or lockable float valve because core orientation and wireline logging were not scheduled for any of the HT sites. Rig floor operations were slowed on the initial pipe trip for several reasons. This was the initial pipe trip of the leg, and the stands of drill pipe had to be measured (strapped) and adequate internal diameter verified (rabbited). A drill string wiper plug (pig) was pumped to remove any loose scale residing in the pipe. In addition, a new driller and assistant driller were being trained. Operations went exceptionally well with no major problems or incidents. The mudline was verified at 5.2 m higher than indicated by the precision depth recorder (PDR). Hole conditions were excellent and no drilling mud was required. Seawater was the only circulation fluid used.

SITE 1024
(Proposed Site HT-3A)

Hole 1024A

After releasing and recovering the beacon at Site 1023 (HT-2A) the ship was moved in dynamic positioning (DP) mode using differential Global Positioning System (dGPS) to the location coordinates for Site 1024. A single piston core was taken only to define mudline for the jet-in test. The mudline was verified to be 7.1 m higher than the PDR indicated. A jet-in test was conducted to 38.5 mbsf in 55.5 min, using up to 22 spm. This information was used to determine the amount of 16" casing (conductor pipe) to be deployed with the reentry cone on Hole 1024C.

Hole 1024B

The ship was offset in DP mode 500 m to the south-southwest before spudding Hole 1024B. The hole was located as far as possible from the coordinates of the primary CORK hole. The move was made with the drill pipe suspended on knobby drilling joints through the guide horn and the bit a minimum 100 m above the relatively flat seafloor. Based on the APC spud core, the mudline was verified 7.5 m above that indicated by the PDR. Hole conditions were again excellent and no drilling mud was required. The hole was displaced with weighted (10.5 lb/gal) gel mud after reaching basement depth. Operations went exceptionally well with no major problems or incidents.

SITE 1025
(Proposed Site HT-4A)

Hole 1025A

After the beacon at Site 1024 was released and recovered, the ship was moved in DP mode using DGPS to the coordinates for Site 1025. A single piston core was taken to define the mudline for the jet-in test. The mudline was verified to be 6.2 m higher than the PDR indicated. A jet-in test was conducted to 39.7 mbsf using up to 60 spm and completed in 3 hrs and 18 min. This information was used to determine the amount of 16" casing (conductor pipe) to be deployed with the reentry cone on Hole 1025C.

Hole 1025B

The ship was offset in DP mode 500 m to the south-southwest before spudding Hole 1025B. The hole was located as far as possible from the coordinates of the primary CORK hole. The move was made with the drill pipe suspended on knobby drilling joints through the guide horn and the bit at a minimum 100 m above the relatively flat seafloor. Based on the APC spud core, mudline was verified 3.9 m above that indicated by the PDR. Hole conditions remained excellent and no drilling mud was required. The hole was displaced with weighted (10.5 lb/gal) gel mud after reaching basement depth. Operations went exceptionally well with no major problems or incidents.

Hole 1025C

Prior to spudding Hole 1025C the ship was moved in DP mode back 500 m to the original coordinates for Hole 1025A. A reentry cone and 16" conductor pipe were deployed and washed into the seafloor without incident. The 16" casing shoe was placed at 2657.4 meters below rig floor (mbrf) (40.2 mbsf). The Dril-Quip 16" running tool was released from the reentry cone/casing. The running tool was dressed with the CADA option allowing the 14-3/4" tricone drill bit to be advanced downhole. A 14-3/4" hole for the 10-3/4" surface casing string was drilled to 106.1 mbsf (5.1 m into basement). Two meters of hard fill were found in the hole after picking up the drill string for a connection. Drilling progress slowed noticibly at that point, and it was decided not to pursue deepening the hole farther. The hole was flushed with a 30 bbl sweep of sepiolite mud, and the bit was pulled to 2644.0 mbrf (up inside the 16" conductor casing). To allow time for any fill to settle in the hole, the top drive was set back and the drilling line was slipped and cut. Approximately 2.5 hr later the second half of the wiper trip was begun. The pipe was run to the original total depth (TD) of 2723.3 mbrf (106.1 mbsf) without any resistance. Encouraged by the apparent stability, we left the hole filled with seawater and the drill string was tripped back to the surface. A 98.8-m-long string of 40.5 lb/ft 10-3/4" K-55 casing was then made up and run to bottom. Reentry took 1 hr partially because of obscured vision from sediment clouds emenating from the reentry cone. Once the hole was reentered, the casing went smoothly downhole without any problem. Approximately 4 m short of landing the casing hanger, the drill pipe was hung off at the rotary table. The top drive was picked up along with the TIW subsea-release cementing manifold and a 30 ft knobby drilling joint. With the heave compensator activated, the 10-3/4" casing hanger was landed and latched. A 10,000 lb tension was taken on the hanger to verify proper latch-in. With the 10-3/4" casing shoe placed at 2718.7 mbrf (101.5 mbsf), 44 bbl of 15.8-ppg class G neat cement were mixed and displaced around the casing shoe. With a 5,000 lb tension applied, the drillstring was rotated 3-1/2 turns to the right. After a few minutes of working the pipe and releasing the torque buildup, the Dril-Quip running tool spun freely. A 12,000 lb weight loss indicated that the casing was free of the drill string and the pipe was tripped back to the surface. The drill floor was secured for transit, the positioning beacon was commanded off, and the vessel then got underway for proposed Site PP-5A (Site 1026). Operations moved to the RB area to allow the cement ample time to cure and, thus, to increase the chance for a better seal. This strategy was used for all the cased holes in which a CORK was installed, which enabled us to use the time spent waiting for cement to cure to complete coring and casing at nearby holes.

SITE 1026
(Proposed Site PP-5A)

Hole 1026A

The 3.5 hr transit to Site 1026 was brief and uneventful. Once the beacon was deployed, the pipe was run to bottom and APC coring commenced. The first core recovered 5.41 m, which established the mudline 3.3 m higher than the PDR indicated. The hole was cored to APC refusal (as defined in this hole by failure to fully stroke). Adara temperature measurements were taken on every other core beginning with Core 168-1026A-4H. Drilling operations were routine with no major problems or incidents. Seawater was the only circulation fluid used during the coring operation. The hole was displaced with heavy mud (10.5 lb/gal) prior to abandonment. After clearing the seafloor with the drill bit, a jet-in test was conducted to determine the amount of 16" casing (conductor pipe) to be used with the reentry cone for this site. The beacon was left on bottom and turned on, because the site was to be reoccupied relatively soon.

SITE 1027
(Proposed Site PP-4A)

Hole 1027A

The drill ship was offset 1.2 nm to Site 1027 in DP mode with the drill string suspended in the same manner as on the other DP moves this leg. Based on earlier mudline depths, the bit was positioned 6.4 m above the PDR depth for the first spud attempt. Sediment was penetrated, but the first core barrel recovered was empty; the core had fallen out of the liner, and, thus, it was impossible to identify a mudline depth. A second attempt at spudding was made from the same depth, and this time a full core (9.92 m) was recovered. The hole was abandoned again for lack of a positive mudline identification. The hole was logged as an official hole (1027A) because the core material was curated and kept for further analysis by the shipboard geochemists.

Hole 1027B

After a successful mudline core was recovered, coring in Hole 1027B continued through Core 168-1027B-62X. Basalt pebbles were first identified in Core 168-1027B-60X and became more predominant with each successive core. The hole was terminated at a depth of 3246.2 mbrf (577.9 mbsf) when it was decided not to spend any more time searching for "absolute" basement. Sepiolite mud sweeps of 25 bbl each were circulated approximately every 40-60 m to aid in hole cleaning. Despite high sand content in the upper formation, the hole remained stable to TD. There was no indication of fill after pipe connections and no increase in pump pressure or drilling torque as the hole proceeded. Once coring operations were concluded 25 bbl of 15.8-ppg cement were placed in the hole and the remainder was displaced with heavy mud.

A total of four Adara temperature measurements were taken in Hole 1027B. The DVTP was deployed 18 times. Tool 1 failed during recovery (after Core 168-1027B-40X). The data were ultimately recovered but are not a good measurement.

Hole 1027C

The ship was offset in DDP mode 50 m south-southwest and a jet-in test was conducted to a depth of 40.0 mbsf. A total of 1 hr 52 min was required for the test at a maximum of 50 spm and 10,000 lb weight. After recovering the drill string, a reentry cone with 16" casing was made up and deployed. The cone landed at the seafloor after jetting the casing shoe for 2 hr 39 min at up to 52 spm and using 20,000 lb weight. The 16" casing shoe was placed at 2704.9 mbrf (37.6 mbsf). The 16" Dril-Quip running tool was released and the drill string was tripped back to the ship. A 14-3/4" tricone bit and drilling BHA was then made up and tripped to bottom. The cone was reentered at 0150 hr on 8 July 96. A 14-3/4" hole was control-drilled to a depth of 3252.1 mbrf (584.8 mbsf) or 9.3 m into basement (575.5 mbsf). A wiper trip was made to the 16" casing shoe and back with minor overpull and drill pipe drag in spots. An apparent ledge was identified approximately 1 m into basement, and the bit was worked through this area several times. Tight hole and light fill characterized the lower 15 m. Without setting back the top drive, a short (six stand) wiper trip was made, and the hole was circulated clean and then displaced with sepiolite mud. The drill string was recovered and 41 joints of 10-3/4" casing were made-up and deployed using the Dril-Quip running tool. After we returned to the seafloor with the casing and searched for several hours, it became apparent that the reentry cone had sunk significantly below the mudline. The cone/16" casing became undermined during the drilling of the 14-3/4" hole. It is theorized that a combination of circulation and vibration fluidized the heavily sand-laden sediments in the upper portion of the hole, allowing the cone to sink 8.3 m below the mudline. Without seeing the cone, the hole was reentered using sonar and the 10-3/4" casing string was deployed until it landed firmly at a depth of 3252.05 mbrf, essentially the hole TD. The string was picked up, to no avail, three times in an attempt to verify that the casing hanger had engaged. The casing shoe was set down one last time while spotting 56 bbl of neat cement around the casing shoe. When the drill string was raised the final time, to everyone’s surprise the reentry cone and 16" casing string came up with it. The reentry cone mudskirt was placed 2 m below the original mudline at a depth of 2669.3 mbrf. This positioned the 16" and 10-3/4" casing shoes at 2704.9 mbrf (38.6 mbsf) and 3245.7 mbrf (578.4 mbsf), respectively. The 10-3/4" shoe was cemented 2.9 m into basement and the entire rathole below the shoe was also filled with cement. Drill string tension was maintained for 12 hr to support the weight of the cone and casing strings while the cement hardened to an acceptable state. The 10-3/4" Dril-Quip running tool disengaged without incident. The cone was left stable and the surface sediments appeared to have backfilled into the cavity up to the bottom of the reentry cone mudskirt. Once the drill string was recovered to a safe depth, the positioning beacon was commanded off and the vessel began moving in DP mode back to Site 1026 (PP-5A).

SITE 1026
(Proposed Site PP-5A)

Hole 1026B

The ship arrived back at Site 1026 before the drill string was completely recovered. The positioning beacon was commanded back on. The Dril-Quip 10-3/4" running tool was detorqued and the drilling line was slipped and cut before preparations began for deployment of the third reentry cone of the leg. After three joints of 16" casing were made up, the reentry cone and casing were deployed to the seafloor. Weather conditions were beginning to deteriorate at this point, so one stand of drill collars above the running tool was left out to facilitate getting the reentry cone through the surge zone of the moon pool as quickly as possible. The cone/casing were deployed to the seafloor. The jetting process required a total of 4 hr 9 min, with circulation rates of up to 51 spm and weights of 25,000 lb. The cone base plate landed solidly at the appropriate mudline depth (2669.1 mbrf) and the 16" Dril-Quip running tool was released routinely. After the drill string was recovered, the 16" Dril-Quip running tool was detorqued at the rig floor and the dart was loaded in the cementing swivel in preparation for later cementing operations. A 14-3/4" BHA was made in just a few minutes and the bit was run to the bottom of the jetted 16" casing. A total of 7.5 hr was required to drill the 14-3/4" hole to a firm basement depth of 2916.2 mbrf (247.1 mbsf). Another 3.25 hr of basement drilling brought the hole to a total depth of 2925.1 mbrf (256.0 mbsf). The hole was flushed with 40 bbl of sepiolite, and a wiper trip was made up into the 16" casing shoe. To allow time for the hole to stabilize and/or for cuttings to settle out, the subsea camera was deployed to inspect the condition of the reentry cone. The inspection indicated that the cone was in good condition, resting at the seafloor as designed. After recovering the camera, the pipe was run back to TD, where 20 m of loose fill was identified on bottom. The fill was circulated out to within 1 m of total depth without requiring rotation of the drill string. Another 40 bbl sepiolite mud sweep was pumped followed by a seawater spacer and enough sepiolite to displace the hole. The drill string was brought back to the surface and preparations were begun for making up 18 joints of 10-3/4" casing. This process was slowed somewhat by significant vessel motion, but was still completed safely and in timely fashion. The 10-3/4" casing string was deployed to the seafloor and, in spite of 1-2 ft heave conditions, the reentry was made in 45 min. The casing string was run to bottom without any resistance and latch-in was verified with 10,000-lbs overpull. The sepiolite in the hole was displaced out and 49 bbl of 15.8-ppg class G neat cement were pumped downhole. The subsea release (SSR) plug was released at 2800 psi and the cementing dart was landed at 1000 psi. Attempts to release the Dril-Quip running tool were unsuccessful, however, when the casing hanger and casing string appeared to be rotating with the running tool. At 1700 hr it was decided to wait and let the cement harden rather than risk compromising the cement bond and seal with the formation. After waiting on cement for 4 hr, the shipboard cement samples were checked and it was decided that another 2-4 hr should be allowed before attempting to put torque into the running tool. At 0300 hr on 15 July 96, another attempt was made at releasing the running tool.

This time the running tool released properly and the drill string was recovered aboard ship. Once secured, the vessel got underway in DP mode back to reentry Site1027.

SITE 1027
(Proposed Site PP-4A)

Hole 1027C

While the ship was moving to Hole 1027C, an attempt to detorque the 10-3/4" Dril-Quip running tool was made at the rig floor. This was only partially successful because of the large amount of fine sand that had infiltrated the mechanism.

The drill string with an RCB BHA was run in the hole with a center bit installed for drilling out the rubber cementing dart, casing shoe, and wiper plug. Reentry was made swiftly (<15 min) and the bit was run to bottom. The cement was tagged at 3234.7 mbrf (567.4 mbsf) and it took a total of 5 hr to completely drill out to the original TD of 3252.1 mbrf (584.8 mbsf). Continuous RCB coring continued from that depth through interbedded basalt flow units, mudstones, and highly altered basal sediments. Some overpull and torque were experienced during coring, but, in general, hole stability was good. No drilling mud was used while coring below the 10-3/4" casing shoe. The hole was eventually terminated in altered pillow basalt. The subsea TV was deployed on the VIT sleeve to inspect the reentry cone for sediment and cuttings. The cone was found clean and, thus, no jetting was required on the way out of the hole. A short wiper trip back to bottom indicated that the hole had 2.0 m of fill. This was circulated out and the drill bit was pulled clear of the reentry cone. Once secured, the ship was moved in DP mode back to Hole 1026B.

SITE 1026
(Proposed Site PP-5A)

Hole 1026B

While the VIT sleeve was being deployed at Hole 1026B the subsea TV system went down, requiring 45 min to repair. The problem was traced to power supply filters installed in surface equipment in the DP control room. With the TV problem corrected, the reentry took place in short order (<15 min). The bit was run to bottom, tagging the cement at 2910.0 mbrf (240.9 mbsf). It took 5.5 hr to drill out the cement and shoe hardware, including recovery of the center bit. Continuous RCB coring proceeded to a depth of 2964.3 mbrf (295.2 mbsf). Coring was plagued with major hole problems. High torque, overpull, and high pump pressure were common. Recovery was extremely poor in the fresh, highly fractured basalt. Recovery consisted primarily of rubble with few cored pieces. Several mud sweeps totaling 160 bbl were circulated while attempting to clean and stabilize the hole. The more the hole was fought, the more unstable it became. Concerns over permanently sticking the drill string eventually led to the termination of coring. The last tag with drill pipe, using no rotation or circulation, indicated a final hole TD of 2939.0 mbrf (269.9 mbsf), or 25.3 m shallower than the maximum depth achieved during coring. The drill string was recovered and packer operations commenced. All pressure piping and manifolds were tested for leakage, and a wiper plug was pumped downhole to ensure that any loose rust would not infiltrate the packer setting go-devil.

After a pipe trip and reentry, the TAM (manufacturer) packer was run to the bottom of the 10-3/4" casing string. Prior to setting the packer, the wireline was run to bottom with the DVTP to get a bottom-hole temperature and to check the hole TD. The depth check indicated that the hole had continued to deteriorate; the fill level was now up to 2929.0 mbrf, or only 4 m below the depth of the rathole. A temperature measurement at TD indicated that the hole seemed to be losing fluid at a slow rate. Once inside the casing, the TAM packer was set at 2878.1 mbrf. Two slug tests and two injection tests were conducted. Early results indicated that the formation was slightly underpressured. Possible fluid loss through the formation or past the casing cement was also suspected. Upon completion of the packer experiments, the drill string was pulled clear of the reentry cone. The pipe was secured and the ship moved in DP mode back to Hole 1027C for additional packer work.

SITE 1027
(Proposed Site PP-4A)

Hole 1027C

After moving back to Hole 1027C (PP-4A) in DP mode, the hole was reentered and the pipe was run to one stand above the 10-3/4" casing shoe. At that point the wireline sinker bars were deployed with the DVTP tool. A depth check of the hole indicated that the hole depth had remained stable and no further fill had entered. A bottom-hole temperature measurement was also taken at that time. The TAM packer was set twice. The first set was inside the casing at 3228.0 mbrf. Three slug tests and two injection tests were conducted on the first set. The second packer set was in open hole at 3258.0 mbrf (590.7 mbsf). Two slug tests and three injection tests were conducted on the second packer set. Early results indicated that the formation may again be slightly underpressured. The testing went exceptionally well and the data appear to be of good quality. After completion of packer experiments, the drill string was recovered and preparations were begun in calm seas for the first CORK deployment of the leg. Deployment of the CORK, data logger, and osmotic sampler systems went well and there were few problems. The CORK running tool was difficult to align with the CORK body because of their massive sizes. Once this was done and the mating surfaces were coated with pipe dope, the tool slid on easily. The thermistor string was lengthened by 15 m to take advantage of the extra hole depth. While the drill string was being recovered, the positioning beacon was released/recovered and the ship began moving in DP mode back to Hole 1026B (PP-5A) for final CORK operations at that site.

SITE 1026
(Proposed Site PP-5A)

Hole 1026B

Before the drill string was fully recovered, the move in DP mode to Hole 1026B was completed. The CORK running tool was set aside and preparations were begun to deploy a drill-in liner assembly made up of a modified mechanical bit release (MBR) and seven joints of junk 5" drill pipe. The pin connection was cut off the MBR bit disconnect. The box end of the top joint of 5" drill pipe was then slipped on and welded. Stabilizer pads were welded onto the MBR body and turned to the drift diameter of the 10-3/4" casing. This assembly was run in the hole and the cone was reentered. The level of fill in the hole was tagged with the pin end of the drill-in liner at a depth of 2929.0 mbrf (259.9 mbsf). This was 35.3 m above the original hole TD and only 12.8 m into basement (2916.2 mbrf). It was hoped that by drilling/washing in the drill string liner a conduit would be provided farther into basement for the thermistor string. Because of the poor hole conditions, it was considered unlikely that the hole would ever be deepened in the future. After multiple attempts, the liner was eventually worked down to a depth of 2955.0 mbrf (285.9 mbsf) using very slow rpm (5) and very low circulation (20 spm). Drilling torque was 75-100 amps. Heavy mud was spotted in the drill string to keep the flow moving in a downward direction during connections. We tried to get the liner in place with the least disturbance or vertical displacement of the fill up the annulus outside the liner. It was feared that if they were highly fluidized, cuttings could flow back into the liner from the bottom or if displaced high enough would spill over the top of the liner. The rotary shifting tool and sinker bars were installed during the last connection, making the release operation relatively straight forward. Once the MBR was released, the annulus was circulated clean and the heavy mud was displaced out of the annulus using seawater. The shifting tool was recovered and the sinker bars were run back to bottom to check the depth of open hole. On the first tag, 4.0 m of fill was found inside the drill pipe liner at a depth of 2951.0 mbrf. After waiting 1 hr for cuttings to settle out further, the fill was again checked. This time the fill had reached a depth of 2949.0 mbrf, or 7 m up inside the liner. The final hole depth available for thermistor deployment was left at 31.8 m into basement. Nearly 20 m of open hole had been regained by this effort. The top of the liner was placed at 2887.0 mbrf, or 30.6 m above the 10-3/4" casing shoe. By the time the drill string was recovered, weather conditions were marginal for a CORK deployment, and the forecast indicated that weather and sea-state conditions would likely continue to deteriorate over the next 12-18 hr. As a result, the CORK deployment was deferred until later in the leg. The ship was secured and departed for Hole 1024C, where the last cone/casing deployment of the leg was to be made.

SITE 1024
(Proposed Site HT-3A)

Hole 1024C

Because of poor weather conditions, we had to delay installation of a CORK at Site 1026. Therefore, we decided to move back to Site 1024 and set what had become the fourth reentry cone of the leg, in preparation for installing a CORK. After preparation, a cone with 16" conductor pipe was run to bottom. The jetting operation required a maximum of 46 spm and was completed in 2 hr 44 min. With the reentry cone landed at the mudline, the 16" casing shoe was placed at 2662.5 mbrf (39.2 mbsf). The Dril-Quip 16" running tool was easily released from the reentry cone and casing. The drill string was recovered, the 16" Dril-Quip running tool was detorqued at the rig floor, and a 14-3/4" drilling assembly with a tricone bit was made up. The assembly was lowered to the seafloor, and after deploying the VIT, a routine reentry was made in 30 min. The drilling rate to basement was fairly rapid at first. Drilling continued at an average rate of penetration (ROP) of 30 m/hr until a depth of 2775.0 mbrf (151.7 mbsf) was reached. After the drilling break, the ROP slowed to 1-2 m/hr until TD was reached at a depth of 2797.0 mbrf (173.7 mbsf), 22.0 m into hard rock. In the lower part of the hole, the drilling was characterized by high torque and some pipe sticking, but only on bottom. The drilling parameters rapidly returned to normal once the bit was lifted off bottom. At the conclusion of drilling, the hole was circulated with seawater and a wiper trip was made to the 16" casing shoe. During the return trip, fill was tagged 16 m off bottom. This was easily circulated away until firm fill was reached 7.6 m above the original TD. An additional 2.0 m was washed away and then a 40-bbl sepiolite mud sweep was pumped. After a short trip, fill was still evident 10 m off bottom. The top drive was used to circulate the fill out until hard fill was reached 3.0 m above TD. At this point another 50-bbl sepiolite pill was circulated followed by a 50-bbl seawater spacer and 140 bbl of sepiolite mud to displace the hole. The drilling assembly was recovered and preparations were begun for making up and running the 10-3/4" surface casing string. It took only 3.5 hr to make up 12 joints of K-55 40.5-lb/ft surface casing including making up the casing hanger, Dril-Quip running tool, etc. After the casing was run to the seafloor, the top drive and TIW cementing manifold were picked up and within 45 min another reentry was made. The casing hanger was landed and latch-in confirmed with 15,000-lb overpull. A total of 61.7 bbl of 15.8-ppg class G neat cement was mixed and displaced downhole; however, there was no indication that the dart landed or that the wiper plug released properly. Although the Dril-Quip running tool appeared to rotate downhole the requisite number of turns (3.5 to the right) the tool would not come free from the hanger. After waiting nearly 6 hr for the cement to partially harden, the pipe was merely raised and the tool came free. Apparently the tool did rotate properly, because the buoyancy effect of the casing in the cement put the release ring in compression, preventing the ring from moving inward to release. A higher overpull applied earlier probably would have released the tool at that time. The drill string was tripped back to the drill ship, ending the present round of operations at Hole 1024C. This hole was to be reoccupied later for RCB coring in basement, packer experiments, and CORK setting.

SITE 1025
(Proposed Site HT-4A)

Hole 1025C

The drill ship was offset in DP mode back to Hole 1025C while recovering the casing running BHA from Hole 1024C (HT-3A). The 10-3/4" Dril-Quip running tool was detorqued at the rig floor and an RCB BHA with mechanical drilling jars was made up and run in the hole. The reentry cone was reentered 15 min after reaching the seafloor, and the drilling assembly was run to bottom. The top of the cement was tagged at a depth of 2706.0 mbrf (88.8 mbsf). Just under 6 hr was required to drill out the cement in the casing, casing shoe, and cement beneath the shoe. The center bit was recovered on the wireline and RCB coring operations commenced. Continuous RCB coring in igneous basement progressed through Core 168-1025C-5R to a total depth of 2764.4 mbrf (147.2 mbsf) with moderate recovery. The rate of penetration varied significantly as various units within basement were penetrated. Drilling was slow in massive layers; some zones were encountered where the bottom seemed to fall out and rapid penetration was achieved for several meters. Hole conditions were generally good, although some pipe sticking and hole trouble became apparent after advancing Core 168-1025C-4R to a depth of 2754.8 mbrf (137.6 mbsf). The tight spots were worked repeatedly with the drill pipe, and 30-bbl sepiolite mud sweeps were pumped after Cores 168-1025C-4R and -5R. A wiper trip to 108.9 mbsf was made, and on the return trip ledges in the hole were identified at 2725.0 mbrf (107.8 mbsf) and 2746.0 mbrf (128.8 mbsf). Fill was tagged at 2749.0 mbrf, 15.4 m off bottom. Another 30-bbl sepiolite mud sweep was pumped while washing back to TD. On the next short trip, fill was tagged at 2756.0 mbrf, or 8.4 m off bottom. The fill was circulated out one last time, and a 30-bbl sepiolite mud sweep was pumped. The drill string was recovered and preparations for deployment of the TAM packer were initiated. Once reentry was accomplished with the TAM packer (30 min), the BHA was run to the packer setting point inside the second casing joint from the bottom. A wireline depth check of TD was made before beginning packer operations to determine the amount of hole available for thermistor emplacement. The DVTP was deployed and measurements taken at 5.0-m intervals from the 10-3/4" casing shoe to TD during the first depth-check wireline run. A temperature profile of the hole was obtained. Hole depth was measured at 2754.0 mbrf (136.8 mbsf), or 35.8 m into basement. Several unsuccessful attempts were made to set the TAM packer. Multiple wireline runs were made with the first setting go-devil, and another go-devil was used as well. Nothing was wrong with either go-devil yet the packer would not inflate. Another depth check of the hole was made using the wireline while meeting with rig personnel, co-chiefs, and packer scientists. It was decided that further attempts to perform packer operations would be abandoned in lieu of proceeding with setting the CORK assembly. Two compelling factors affected the decision. The current weather window was ideal for CORK setting and the second wireline depth check indicated another possible loss of 2.0 m of hole (TD 2752.0 mbrf). The measurements were made about 6 hr apart and could have been partially influenced by the 2.0-m tide that was apparent for most of the leg; however, there was continued concern about additional loss of available hole for thermistor deployment. The drill string was tripped back to the rig floor and preparations for setting the second CORK were begun.

Upon inspection, no mechanical problems were found with the packer assembly. A new control sleeve was installed after the last deployment. The new sleeve apparently fit somewhat tighter than the old worn one. With little or no weight below the packer, the new control sleeve apparently stopped approximately 1" from being fully extended in the open position. If the control sleeve is not fully open, inflation cannot take place and setting the packer becomes impossible.

Obsolete 9-1/2" drill collars (three each) were used for CORK stinger material. These were too large for the iron roughneck to handle, so conventional rig tongs were used for make up. Rig-up and deployment of the CORK assembly went well without major problems. The CORK was tripped to the seafloor and reentry was made within 10 min. The stinger was positioned inside the reentry cone without landing the CORK and the thermistor string/osmotic pump assembly was deployed down the drill string. As with the first CORK deployment at Site 1027, the dual-grip lifting technique was used. This system is less than ideal, but it worked well enough for the relatively short thermistor string. Within 1 hr the thermistor was deployed inside the drill pipe and ready for running to bottom. A final electronic check was made on the data logger located at the top of the thermistor string and the assembly was run to bottom on the wireline using the setting tool of the datalogger. Several landing attempts were made to seat the seals before the release tool would pressure up. The shear pin in the overshot apparently sheared during the pressurization phase, because no overpull was experienced when recovering the wireline. The

CORK setting go-devil was deployed after pulling the mousehole and picking up two additional joints of drill pipe. The CORK was landed and the setting go-devil pressured up. Latch engagement was verified with drill string overpull and the CORK platform was deployed. The subsea TV was deployed to verify that the installation was complete. The CORK running tool was released and the camera was recovered. The drill string was tripped back to the rig floor and the positioning beacon was recovered. During the trip out, the ship was offset in DP mode back to Hole 1024C. The hole was ended once all tools were recovered back aboard ship.

SITE 1024
(Proposed Site HT-3A)

Hole 1024C

An RCB BHA was made up and run to the seafloor. The VIT was deployed during the pipe trip and a routine reentry was made within 15 min. The bit contacted the top of the cement column at a depth of 2777.2 mbrf (153.9 mbsf). The cement and float shoe were drilled out in short order, and the center bit was recovered. On this hole the cementing dart and wiper plug did not release. The dart was recovered, but it was not known whether the casing wiper plug fell into the reentry cone or outside the hole. The bit broke through to the rathole after only 1.5 hr. Once RCB coring was initiated, the bit advanced only 2.0 m before tight hole and torquing led to early retrieval of the core barrel. Recovery was minimal (0.12 m), but included in the core liner was a section of the float shoe including the entire float valve assembly. Apparently the inner portion of the float shoe had broken free during the center bit drilling phase and fallen to the bottom of the rat hole. This allowed the core barrel to swallow the float valve perfectly during the first coring attempt. The next 4 hr were spent fighting stuck pipe and hole trouble until the decision was made to abandon attempts at further penetration. Earlier in the leg, while drilling the 14-3/4" hole for the 10-3/4" surface casing, the drilling was also stopped because of bad hole conditions and stuck pipe. The hole was abandoned at that time at 22.0 m into basement and was left with 3.0 m of hard fill on bottom. Coring operations on this bit run were halted after one core and a total TD of 2797.0 mbrf (173.7 mbsf). The depth of open hole remained the same, at 2794.0 mbrf (169.7 mbsf). The bit was pulled up inside the 10-3/4" casing shoe and the second core barrel was recovered. This was not considered a core, because no advance was made and no core recovery was obtained. After tripping the drill string and prior to making up the TAM packer BHA, the mechanical drilling jars were tested at the rig floor. The jars were not only locked up from the debris but also had failed to hold circulation pressure. This undoubtedly contributed to the hole cleaning problems during the attempted coring, because full circulation was obviously not getting to the bit. Because identical drilling problems occurred while drilling the 14-3/4" hole without the drilling jars in the BHA, we did not believe that was the sole reason for the failure to advance the hole. The jars were cleaned up and prepared for shipment back for refurbishment. A reentry cleanout bit and a 10-ft drill collar pup joint were made up directly below the packer to aid in keeping the control sleeve fully extended. The packer BHA was run to bottom, but prior to reentry a wiper plug was pumped down the drill string. After another routine 15-min reentry, the circulation system was pressure tested and the pipe was lowered to a packer setting depth of 2775.3 mbrf (152.0 mbsf). The DVTP was run to bottom on the wireline for a preliminary depth check of the hole and to obtain a bottom-hole temperature. There was no problem setting the packer in this hole, and the packer testing went exceptionally well. After two successful injection and flow tests were completed, the packer was released and a final depth check was made with the wireline. Useable hole depth was confirmed as unchanged at 2794.0 mbrf, and this depth was used to calculate the final thermistor length for the hole. The pipe was retrieved back to the ship and preparations began for deploying the third CORK. The CORK deployment again went exceptionally well. The last of the obsolete 9-1/2" drill collars (three each) were made up as the CORK stinger and hung off. The CORK body was positioned in the skate and the running tool made up. The CORK assembly was made up to the CORK stinger and lowered so the final connection could be made with the CORK setting hose. As on earlier deployments, the hole number was painted on the CORK body identifying the installation for later visits by submersible or remote-operated vehicle (ROV). Once the safety blocks and packing protectors were removed, the CORK was ready for deployment. The tool was run to bottom, and within 15 min a reentry was made. Deployment of the osmotic sampler, thermistor string, and data logger proceeded without incident. A final electronic check on the data logger was conducted just prior to installing the running tool. The thermistor string was run to bottom and the data logger landed/latched into the CORK. A wireline overpull, before shearing the weakened overshot pin in the running tool, confirmed data logger latch-in. After retrieving the wireline, the CORK setting tool was deployed and pressured up. After bleeding off the pressure, the drill pipe was picked up, and a 10,000-lb overpull confirmed that the CORK was now latched in place. The VIT frame was deployed and the subsea TV was used to witness the release from the CORK installation. The setting go-devil was retrieved and the drill string was tripped back to the ship while the positioning beacon was released and recovered. Once the ship was secured, the hole was officially ended and the transit to Hole 1026C was begun.

SITE 1026
(Proposed Site PP-5A)

Hole 1026C

After the completion of the CORK operations at Sites 1024 and 1025, the ship was secured and headed to Site 1026 to complete the fourth and last CORK installation and to core the lower part of the sediment section. During the 5-hr transit back, the ship was slowed to 6 kt to test a new seismic streamer. Once the test was completed, the ship resumed full speed. Hole 1026C was located approximately 1000 m from Hole 1026B, at N17°E, but was geologically considered part of the same sequence of holes at Site 1026. A beacon was dropped and an RCB BHA was made up and tripped to bottom. The RCB system was used because there was higher interest in recovering indurated sediment and basement samples rather than the softer overlying sediments. Because the upper 101.4 m of sediment had already been piston cored at Hole 1026A, the top 84.6 m was drilled with a center bit. Continuous RCB coring began at that point and continued to a depth of 248.2 mbsf. Recovery was poor until nearly 210 mbsf, where the sediments were finally indurated enough for the RCB system to be effective. The last three sediment cores achieved 90% recovery. Two subsequent basement cores in basalt rubble again failed to recover any "cored" material providing only pieces of rubble "rollers" that tended to jam the core catchers. Some torquing was evident in basement, but was not severe. One meter of fill was detected after making the connection before the last core. Once coring operations were terminated, the pipe was worked back to bottom and a 30-bbl sepiolite mud pill was circulated to try and clean the hole as much as possible. A wireline run was made to release the bit and the hole was plugged with 29.7 bbl of 15.8-ppg class G cement spotted in basement. The cement was required to reisolate basement hydrologically to avoid possible perturbations at the nearest CORK site at Hole 1026B. The bit was then pulled clear of the mudline, and the beacon was recovered to end Hole 1026C.

Hole 1026B

The ship was offset 1000 m back to Hole 1026B, and the hole reentered within 15 min after the rig floor was ready. The pipe was lowered to a depth of 2874.6 mbrf, and after the top drive and a 20-ft knobby joint were picked up, the DVTP was run in on the wireline. A temperature profile of the borehole fluids was recovered as a bonus while running to bottom for a final thermistor string depth check. Fill was tagged at a depth of 2947.0 mbrf. This was considered essentially the same as before, because it was within 1 m of the last measured depth (i.e., within the variation of a 2-m tide). The top drive was set back, and the driller began to trip the drill string back to the ship. Approximately half way into the pipe trip, the evaluation of the temperature data from the last DVTP deployment was completed. The record indicated an influx of warm formation fluids into the hole. This was seen as an excellent opportunity to attempt recovery of pristine basement fluids. Unfortunately, the WSTP tools would not fit through the bore of the CORK assembly. Therefore, the pipe trip was reversed and the driller began to run back to bottom. After deploying the subsea TV camera, another quick reentry was made and the pipe was run to a depth of 2720.8 mbrf. The top drive was again picked up and the WSTP was run into the hole with an Adara temperature measurement shoe made up to the bottom for redundancy. It was determined that the most likely path for fluid flow was up the annulus between the makeshift drill pipe liner installed earlier in the leg and the 10-3/4" casing. Therefore, the water sampler probe was positioned 8 m above the top of the liner. After allowing time for the sampler valve to open and close, a more detailed temperature profile was taken from the liner to the mudline. Measurements were taken every 10 m for 3 min until 20.9 mbsf. Then the measurements were taken every 2.0 m until 9.1 m above the mudline. When the tool was recovered, it was kept on the rig floor until the quality of the data could be confirmed. The tools were deployed a second time because the volume of fluid recovered was inadequate and the memories on both the Adara and WSTP temperature tools ran out before the mudline was reached. The second deployment recovered a large volume of high-concentration formation fluid and the temperature data were completed. The exercise was exceptionally successful, and all concerned agreed that the time was well spent and the data and samples recovered were extremely valuable. By the time the drill string was recovered, weather conditions had begun to deteriorate and the prognosis was for continued 25-30-kt winds over the next 12-24 hr. Because the sea state had already begun to build, it was deemed inadvisable to begin CORK operations. Once again, deployment of the CORK was deferred at Hole 1026B. The ship was secured and then departed for Site 1028.

SITE 1028

Hole 1028A

The 31.0-nmi transit to Site 1028 was made at a speed of 8.4 kt. A couple of hours were spent at reduced speed (6.0 kt) to perform another test of the seismic streamer. Once on site, the beacon was released and an APC/XCB BHA was made up and run to the seafloor. APC coring proceeded to a depth of 108.2 mbsf where four Adara temperature measurements were taken. A maximum overpull of 50,000 lb was recorded with the Adara shoes and of 30,000 lb without any Adara shoes. XCB coring continued to a final TD of 131.5 mbsf. Basement was contacted at a depth of 130.5 mbsf in Core 168-1028A-15X and 1 hr was spent coring basalt with a hard-formation cutting shoe. The DVTP was deployed twice in the XCB-cored interval. The weather moderated significantly, and within 1/2 hr of completing the pipe trip, the ship was underway for Hole 1026B to deploy the fourth and final CORK of the leg.

SITE 1026
(Proposed Site PP-5A)

Return to Hole 1026B

After completion of Hole 1028A, the ship sailed a few hours in calm seas back to Hole 1026B. As on an earlier transit, speed was reduced to 6 kt for a brief period (2 hr) for a second test of the developmental seismic streamer. Once on site, the positioning beacon was turned on and preparations began quickly for deploying the CORK assembly. The entire CORK deployment operation, less the return pipe trip, was completed in only 14 hr. This includes the trip to the seafloor (2669.1 mbrf) with the CORK assembly, handling of the osmotic sampler, deployment of 277.5 m of thermistor cable, final attachment and electronic check of the data logger, deployment and latching of the thermistor assembly (confirmed with 5-kips wireline overpull), landing and latching of the CORK assembly (confirmed with 10-kips drill pipe overpull), recovery of the CORK setting go-devil, deployment of the CORK ROV platform, VIT deployment, release of the CORK running tool, and VIT recovery. The only negative factor to the final CORK operation was that the lower portion of the CORK setting go-devil backed off during recovery and was lost on the seafloor. While storing the CORK tools and securing the rig floor for transit, the four lower guide horn (LGH) cables (three, each broken) were removed from the moonpool area, so that new cables could be fabricated before arrival in Victoria. The upper guide horn (UGH) was installed and the ship got underway for the first (Site 1029) of several alternate sites to be cored during the remaining operational time.

SITE 1029

Hole 1029A

After completion of Site 1026, the ship sailed for 2.5 hr to Site 1029. The BHA was made up and run to bottom for a routine APC/XCB cored hole. The driller tagged bottom while advancing to the APC shoot depth. Accordingly, the bit was picked up 5 m and Hole 1029A was spudded. The seafloor depth was established at 2664.0 mbrf, or 7.4 m above the PDR depth. Coring proceeded for 12 APC cores during which five Adara temperature measurements were taken. APC coring was terminated as a result of incomplete strokes and an overpull of 100,000 lbs was reached. The XCB system was used to deepen the hole with excellent core recovery until basement was tagged at a depth of 2883.5 mbrf (219.5 mbsf). The hole was terminated at 2887.0 mbrf (223.0 mbsf) after coring basement for 1 hr. The drill string was recovered to approximately 100 m above seafloor and the beacon was released/recovered. With knobby drilling joints installed through the guide horn area, the ship began moving to Site 1030.

SITE 1030

Hole 1030A

Hole 1030A was located on a ridge crest with approximately 30 m of sediment cover overlying basement. A positioning beacon was deployed and the drill string was spaced out for initiating drilling operations. A wash test was conducted to avoid hitting basement with the APC and to allow optimal placement of the DVTP for a temperature measurement as close as possible to basement. With a core barrel in place, the drill string was lowered while circulating at a slow rate until the mudline was tagged at a depth of 2589.0 mbrf. Circulation and rotation were kept at a minimal rate until reaching a perceived basement depth of 2628.0 mbrf (39.0 mbsf). The drill string was pulled clear of the mudline and the vessel was offset 10 m for spudding Hole 1030A. The drill string was spaced out for shooting the first APC core from a depth of 2586.0 mbrf, or 3.0 m above tag depth. The spaceout was cut closer than normal, because the scientists desired a minimum 6.5 to 7.0 m of core recovery on the mudline core. This was to be used for chemistry analysis, which would determine the location of the next site. Two potential sites were under consideration after coring Site 1030, and the deciding factor was the chemical analysis from Hole 1030A. When the first core was recovered, it was full, indicating a missed mudline depth. The core was curated as a "wash" Core 168-1030A-1W and coring was halted after this single core. The pipe was then pulled clear of the mudline, ending Hole 1030A.

Hole 1030B

The bit was placed at 2579.0 mbrf, or 7.0 m higher for spudding Hole 1030B. No offset in DP mode was made between holes. This time, 4.01 m was recovered in the first core, establishing the mudline at 2584.5 mbrf. Continuous APC coring continued through Core 168-1030B-5H to a depth of 2625.5 mbrf (41.0 mbsf). The DVTP was then deployed for a single temperature measurement close to the top of anticipated basement. A single XCB Core 168-1030B-6X was then cored through the remaining sediment and into basement. The drillers basement tag depth was 2631.4 m (46.9 mbsf). The drill string was pulled clear of the sea bed and secured at a depth of 2469.4 mbrf (approximately 100 m above the seafloor) with knobby drilling joints through the guide horn. The beacon eventually released after multiple transmissions and was recovered aboard ship. This was the first and only beacon problem experienced during the leg. Once the beacon was secured, the ship began to move in DP mode to Hole 1031A approximately 1000 m away.

SITE 1031

Hole 1031A

The DP move to Hole 1031A was uneventful. Once on location, a positioning beacon was deployed and the pipe was positioned to wash to basement in a manner similar to Site 1030. Jetting was initiated at 1135 hr and the pipe was advanced to a depth of 2642.5 mbrf (65.5 mbsf), where apparent basement was tagged. The pipe was pulled clear of the sea bed, and the ship was offset 10 m west for spudding Hole 1031A. Apparently, the PDR reading was off because of a side echo from a nearby seafloor feature. After two water cores, it was decided to advance the drill string and feel for bottom, and then pick back up for spudding. Two additional single joints were added to the string and seafloor was eventually tagged at ~2602 mbrf. The drill pipe was placed at 2598.5 mbrf, and a mudline core totaling 8.86 m was recovered. APC coring continued through Core 168-1031A-5H with Adara temperature measurements taken on Cores

168-1031A-3H and 4H. The DVTP was deployed after Core 168-1031A-4H. Core 168-1031A-5H impacted basement and recovered approximately 4.0 m of undisturbed core with the remainder of the material flow-in. A single XCB Core 168-1031A-6X was advanced 1.5 m into basement in just under 1 hr, recovering 0.38 m of basement rock. The drill string was pulled out of the hole and the APC/XCB BHA was nondestructively tested as it reached the drill floor. Once secured, the beacon was recovered and the vessel departed for Site 1032 (Proposed Site LH-2).

SITE 1032
(Proposed Site LH-2)

Hole 1032A

The transit to the last site took only 2.5 hr from getting under way to the beacon drop. Hole 1032A was spudded with a mudline tag depth of 2656.0 mbrf. Drilling, with a center bit in place, proceeded to a depth of 2840.5 mbrf (184.5 mbsf). The center bit was recovered and a single RCB core was cut before the first of six DVTP deployments. Continuous RCB coring, interspersed with DVTP measurements, continued to a depth of 2947.2 mbrf (291.2 mbsf), where basement was tagged 1 m in on Core 168-1032A-12R. Basement coring continued to a TD of 2994.4 mbrf (338.4 mbsf, "Site Summary table"). As the hole progressed farther into basement there was increasingly more fill between connections. Three 40-bbl sepiolite mud sweeps and one 40-bbl sweep with high-viscosity gel mud were made during basement coring to aid in cleaning the hole of cuttings. After coring was terminated, a short trip above the basement contact was made and 14 m of fill was identified on bottom. Another 40-bbl sweep was made while circulating to bottom through the soft fill. A wiper trip to 100 mbsf and back to TD was made prior to logging. Two additional 40-bbl sweeps of gel mud were made during the wiper trip and before displacing the hole with 123 bbl of sepiolite mud for logging. The bit was released and the MBR sleeve was reverse shifted. During the second run, the coring line was coated because it was the last wireline run of the leg. The pipe was pulled to a logging depth of 2746.3 mbrf (90.3 mbsf) with 20 and 30-ft knobbies installed. The logging program consisted of three suites. The first run was made with the triple-combination consisting of porosity, density, photoelectric effect, resistivity, and gamma ray (DITE/HLDT/APS/HNGS tools). In addition, the Lamont-Doherty temperature logging tool (TLT) was run. The first suite of logging tools reached a depth of 2938.0 mbrf (282.0 mbsf). This was a disappointing 9.2 m above the basement contact. Efforts were made to go deeper, but to no avail. The caliper logs recovered during this run indicated a fairly good hole through the sediment column (11"-12" hole) but a very ratty hole in the deeper part of the section above basement. The second suite of logs consisted of the FMS and sonic tools (FMS/sonic/NGT). This suite reached a depth of 2933.0 mbrf, or 5 m shallower than the first run. Two passes with the FMS/Sonic tools were made. The third logging suite consisted of the geochemical tool (GST/ACT/CNTG/NGTC). The third deployment reached a depth of 2932.0 mbrf, another meter higher in the hole. Logging was completed by 1900 hr, 14 August 1996. The drill pipe was pulled and the rig floor was secured at 2400 hr, 14 August. The ship set sail for Victoria, BC, with an estimated arrival at 2100 hr, 15 August.

OCEAN DRILLING PROGRAM
OPERATIONS RESUME
LEG 168

Total Days (20 June 96 to 15 August 96)		60.5
Total Days in Port		4.0
Total Days Underway		5.0
Total Days on Site		51.5
	days	
Stuck Pipe/Downhole Trouble	0.7	
Tripping	17.3	
Other	4.6	
Drilling	4.3	
Coring	13.5	
ODP Breakdown	0.1	
Logging/Downhole Science	6.3	
Fishing & Remedial	0.0	
Development Engineering	0.0	
Repair Time (Contractor)	0.0	
Reentry	0.6	
W.O.W.	0.0	
Casing and Cementing	4.1	
Total Distance Traveled (nautical miles)		
Average Speed Transit (knots):		
Number of Sites		10
Number of Holes		19
Number of Reentries		21
Number of Cores Attempted		230.0
Total Interval Cored (m)		2070.6
Total Core Recovery (m)		1571.4
% Core Recovery		75.9%
Total Interval Drilled (m)		1209.6
Total Penetration		3280.2
Maximum Penetration (m)		577.9
Minimum Penetration		6.3
Maximum Water Depth (m from drilling datum)		2669.1
Minimum Water Depth (m from drilling datum)		2584.5
Average Water Depth		2637.1

LEG 168
TOTAL TIME DISTRIBUTION

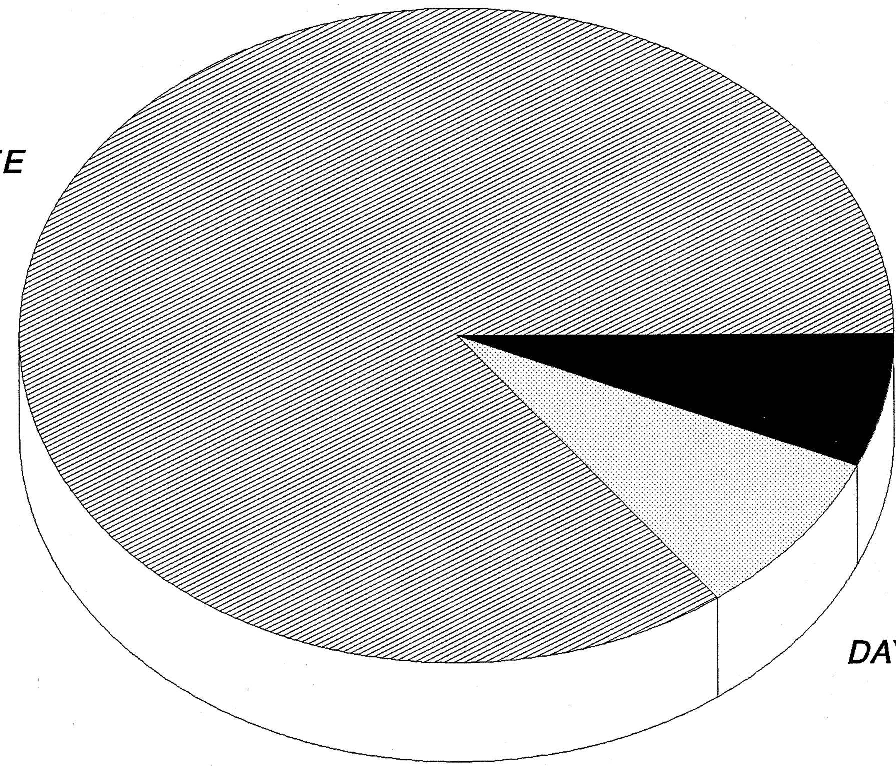

TOTAL DAYS=60.5

OCEAN DRILLING PROGRAM
LEG 168 - SITE SUMMARY

HOLE	LATITUDE	LONGITUDE	SEA FLOOR (mbrf)	NUMBER OF CORES	INTERVAL CORED (meters)	CORE RECOVERED (meters)	PERCENT RECOVERED (percent)	DRILLED (meters)	TOTAL PENETRATION	TIME ON HOLE (hours)	TIME ON HOLE (days)
1023A	47° 55.040 N	128° 47.529 W	2604.2	22	194.5	193.05	99.3%	0.0	194.5	41.00	1.71
SITE 1023 (HT-2A) TOTALS:				**22**	**194.5**	**193.05**	**99.3%**	**0.0**	**194.5**	**41.00**	**1.71**
1024A	47°54.522 N	128°44.975 W	2623.3	1	9.2	9.19	99.9%	0.0	9.2	7.00	0.29
1024B	47°54.274 N	128°45.132 W	2624.9	18	169.6	170.11	100.3%	0.0	169.6	23.75	0.99
1024C	47°54.531 N	128°45.005 W	2623.3	1	2.0	0.12	6.0%	173.7	175.7	159.25	6.64
SITE 1024 (HT-3A) TOTALS:				**20**	**180.8**	**179.42**	**99.2%**	**173.7**	**354.5**	**190.00**	**7.92**
1025A	47°53.247 N	128°38.920 W	2617.2	1	6.3	6.34	100.6%	0.0	6.3	8.75	0.36
1025B	47°52.998 N	128°39.052 W	2624.5	11	99.5	90.98	91.4%	0.0	99.5	20.00	0.83
1025C	47°53.247 N	128°38.919 W	2617.2	5	41.1	15.16	36.9%	0.0	41.1	140.00	5.83
SITE 1025 (HT-4A) TOTALS:				**17**	**146.9**	**112.48**	**76.6%**	**0**	**146.9**	**168.75**	**7.03**
1026A	47°45.757 N	127°45.552 W	2669.1	12	101.4	105.57	104.1%	0.0	101.4	22.25	0.93
1026B	47°45.759 N	127°45.552 W	2669.1	5	39.2	1.95	5.0%	218.6	257.8	213.50	8.90
1026C	47°46.261 N	127°45.186 W	2669.1	17	163.6	49.80	30.4%	84.6	248.2	40.00	1.67
SITE 1026 (PP-5A) TOTALS:				**34**	**304.2**	**157.32**	**51.7%**	**303**	**607.4**	**275.75**	**11.49**
1027A	47°45.412 N	127°43.854 W	2668.3	1	9.5	9.92	104.4%	0.0	9.5	3.00	0.13
1027B	47°45.412 N	127°43.853 W	2668.3	62	577.9	414.91	71.8%	0.0	577.9	121.00	5.04
1027C	47°45.387 N	127°43.867 W	2667.3	5	47.6	29.13	61.2%	548.2	595.8	225.75	9.41
SITE 1027 (PP-4A) TOTALS:				**68**	**635.0**	**453.96**	**71.5%**	**548.2**	**1183.2**	**349.75**	**14.57**
1028A	47°51.479 N	128°30.289 W	2670.8	15	131.5	124.91	95.0%	0.0	131.5	28.00	1.17
SITE 1028 TOTALS:				**15**	**131.5**	**124.91**	**95.0%**	**0.0**	**131.5**	**28.00**	**1.17**
1029A	47°49.901 N	128°22.597 W	2664.0	25	223.0	202.97	91.0%	0.0	223.0	38.00	1.58
SITE 1029 TOTALS:				**25**	**223.0**	**202.97**	**91.0%**	**0.0**	**223.0**	**38.00**	**1.58**
1030A	47°53.847 N	128°33.711 W	2584.5	1	9.5	9.76	102.7%	0.0	9.5	13.25	0.55
1030B	47°53.847 N	128°33.711 W	2584.5	6	48.5	44.11	90.9%	0.0	48.5	9.00	0.38
SITE 1030 TOTALS:				**7**	**58.0**	**53.87**	**92.9%**	**0.0**	**58.0**	**22.25**	**0.93**
1031A	47°53.400 N	128°33.970 W	2599.2	6	42.8	42.56	99.4%	0.0	42.8	24.25	1.01
SITE 1031 TOTALS:				**6**	**42.8**	**42.56**	**99.4%**	**0.0**	**42.8**	**24.25**	**1.01**
1032A	47°46.773 N	128°07.341 W	2656.0	16	153.9	50.86	33.0%	184.5	338.4	84.00	3.50
SITE 1032 (LH-2) TOTALS:				**16**	**153.9**	**50.86**	**33.0%**	**184.5**	**338.4**	**84.00**	**3.50**
LEG 168 TOTALS:				**230**	**2070.6**	**1571.40**	**75.9%**	**1209.6**	**3280.2**	**1221.75**	**50.91**

TECHNICAL REPORT

The ODP Technical and Logistics personnel aboard *JOIDES Resolution* for Leg 168 were

Tim Bronk	Marine Lab Specialist (Chemistry)
Roy Davis	Marine Lab Specialist (Photographer)
Sandy Dillard	Marine Lab Specialist (Storekeeper)
Burney Hamlin	Laboratory Officer
Margaret Hastedt	Assistant Lab Officer (Paleomagnetics)
Terry Klepac	Marine Computer Specialist (System Manager)
Kuro Kuroki	Assistant Lab Officer
Mont Lawyer	Marine Lab Specialist (Underway Geophysics)
Jaque Ledbetter	Marine Lab Specialist (X-Ray)
Greg Lovelace	Marine Lab Specialist (Physical Properties)
Erinn McCarty	Marine Lab Specialist (Curator)
Matt Mefferd	Marine Computer Specialist (System Manager)
Chris Nugent	Marine Lab Specialist (Downhole Tools)
Anne Pimmel	Marine Lab Specialist (Chemistry)
Jo Ribbens	Marine Lab Specialist (Yeoperson)
Bill Stevens	Marine Electronics Specialist
Mark Watson	Marine Electronics Specialst

GENERAL LEG INFORMATION

The 10 sites during Leg 168 were occupied with 19 holes, four of which were cased into basement with reentry cones and “CORKed” and instrumented with thermistor strings and water samplers in the holes. They will be visited in the future by submersibles to download data and change the battery packages.

The sets of holes were close to each other and were completed in several steps. For example, while the cement on one casing string was curing, another hole was drilled deeper, or similar work was done in adjacent holes to reduce the time lost tripping pipe. Packer experiments and CORK placements were best accomplished during minimum ship heave conditions, so weather factors, too, determined when the work was done. It was an ongoing challenge to keep everyone informed of the ship's current operations. Some long transits in DP mode were made between sites when the slow transit time was still less than round trip pipe time.

San Francisco Port Call

After arriving by bus from the hotel, 16 June 1996, the technical staff and scientists waited several hours on the exposed dock for U.S. Customs to clear the ship and personnel.

Contributing to the delay was a problem with the visas of a few scientists. Their visas were not technically correct because of different entry requirements for those entering the U.S. by ship vs. by air.

Crossover between the teams went quickly and work with the technical representatives commenced. The laboratory microscopes were serviced by SERCO and repaired as necessary; a maintenance class was conducted for the photographers and their shore supervisor.

The FISON/ARL representative arrived late and then spent some of the time getting the instrument, which was used little on the previous leg, to operate normally. This was a routine service call.

The Costeck/Carlo Erba representative conducted a short training session for the chemistry specialists on instrument use and support procedures for the CNS instrument. Parts and instructions for bypassing the sulfur portion of the determination, a modification that speeds the results for carbon when there is no interest or little sulfur in the samples, were explained. There was no time to service the instrument to correct minor problems from previous legs.

The forward catwalk door sill was cut to deck level prior to port call to make it easier and safer to move the long and heavy original 2G cryogenic magnetometer unit out of the core lab and to bring its replacement into the lab. The exchange and installation were scheduled to take up to 5 days, but, in spite of a few harried trips to shore, the instrument was ready to test in 4 days. We did not notice initially that the HP Pentium PC provided to control the unit came without documentation or start-up disks.

Annual Performance Evaluations were conducted only for the sea going personnel during the port call. Bob Olivas, supervisor of the Technical and Logistics group, was present for 2 days to review written ship evaluations and to participate in the reviews, as directed by recent policy changes. This required a few of the off-going technical staff to stay over. They assisted in the loading of the two 40-ft containers of recovered cores. With a service call in progress the first day and the interview schedule, those few left to load the containers appreciated this help.

Public relations tours and science interviews were scheduled and conducted for VIPs on Monday and for the general public and educational groups on Tuesday. A tent and ODP displays were set up on the dock to inform and manage the crowd, while nearby dock workers unloaded and slung the reentry cones and other heavy equipment required to accomplish the objectives set for this leg. Visitors often walked right through the roped-off areas, impeding the movement of materials. In addition, union organization on the docks slowed down the movement of materials on and off the ship. The area in the core lab where the new cryogenic magnetometer was being installed was cordoned off. Crossover for the systems managers and JANUS representative and the microscope instruction sessions were disrupted by the numerous tours.

The tours were successfully conducted by scientists from the greater San Francisco Bay area who had sailed previously. An afternoon and evening reception was scheduled on Monday for the VIPs and scientists; the technical staff was invited and many were able to participate.

Under Way

The *JOIDES Resolution* sailed at 9:03 a.m. on 20 June. Navigation tapes with depths and magnetic measurements were recorded on the track from outside the San Francisco's Golden Gate Bridge to the drill sites off the Washington state coast. No surveying of the area was necessary.

Several short (3 to 4 hr) transits were made between drill sites, and on two we took the opportunity to try one of the new solid-state six-channel streamers. An 80-$in.^3$ water gun was deployed and fired. Difficulty with the SUN computers and a2d software resulted in little meaningful seismic information. A power lead in the streamer was thought to have failed, but further investigation hinted that the preamps had failed because of a possible short when the BNC connectors may have touched. The circuit apparently has critical ground requirements. The streamer was removed from the winch and returned to ODP for repair.

There was marginal success using the dGPS service in this area after being assured that this area was covered. A lengthy phone call with a CHANCE technical representative led the underway technician through a diagnostics routine. They determined that (1) one unit had a bad interface and needed to be returned for a replacement, (2) the antennas should be higher and have a less obstructed view of the horizon, and (3) the dGPS satellite is at 20° at this location, which is marginally low.

The last site, Site 1032, was drilled into basement and a suite of logs was generated. The ship was under way at 2400 on 15 August for port call at Victoria, British Columbia. Depths and magnetometer data were collected until the ship entered the Juan De Fuca Strait; navigation collection continued until the ship reached Victoria.

LAB ACTIVITIES

Chemistry Lab

Shipboard analysis of interstitial-water samples on Leg 168 included refractometric analysis for salinity; titrations for pH, alkalinity, chloride, calcium, and magnesium; ion chromatography for sulfate, potassium, sodium, calcium, and magnesium; and colorimetric analyses for silica, phosphate, ammonium, and boron. Atomic absorption spectrophotometry was used to quantify low concentrations of magnesium in pore waters. The boron determination was hampered by a specialty chemical that did not dissolve properly.

Six hundred “osmosis” samples were analyzed for anions and cations on the Dionex. The samples originated from four OsmoSamplers that were deployed with the CORKs. The analyses will be used to help the scientists determine the changes in composition of the input fluid and its rate of diffusion in the sampler over time as it sits in a CORK.

Sediment core samples were analyzed for inorganic and total carbon, using the coulometer and the CNS. Based on their organic carbon content, some samples were selected and analyzed with the RockEval. The system was used to determine S_1, S_2, S_3, and S_4. Carbon dioxide and structural water were determined on selected rock samples using the CNS.

Gas chromatograph 3 was used during this leg to provide real-time monitoring of the volatile hydrocarbons.

Computer Lab

Although Leg 168 was not a high-recovery leg, computer use was fairly heavy, as usual when members of the science party have the luxury of time for data analysis. It is worth noting that more than an average number of PC users sailed this leg, as well as several avid UNIX users. The large number of sites we drilled gave us a good opportunity to test the post-stabilization period build of the JANUS database with all OPERATIONS and CORELOG data entered.

The SUN operating system was upgraded to Solaris 2.5 and the UNIX environment was standardized to mirror the shore systems. Installation of additional and upgraded software on the SUN stations was performed including back-up software, a graphic exchange facilitator and tools to manage users and printers from a interface on the system manager’s SUN and to conserve disk space. An alternate boot disk was also built to allow quick failure recovery.

Several PC viruses were brought aboard. The first one was troublesome just from the standpoint of trying to figure out what was occurring. Virus detection software was then used regularly, which located and removed two more.

A scheduled power outage (for maintenance) during the San Francisco port call apparently precipitated a number of equipment failures, including two power supplies for Black Box media convertors in the Underway Lab and a 1.3-Gb drive (DATBAK on DEWEY).

The FDDI optical cable project is currently on hold. The electronics staff had a full schedule this leg and no time was available for this major effort. The project is presently planned to be completed on a “time-available basis.” The cable ways were surveyed this leg to determine if there is space in the cable ways, available bulkhead penetration openings, and sufficient curve radii are present to accommodate the cable. Deficiencies were noted that could hamper installation when it is started. The information from this survey was given to the system manager.

Core Lab

The core lab was returned to its usual core flow configuration while proceeding to the leg's drill sites. The core drills and sample cutting saws were returned to the aft bench. The core entry bench was cleared to accommodate the tools used to take biological samples.

Curation

Sediment and basalt basement cores were recovered on Leg 168. The fact that these cores were not drilled in sequential order will make racking the cores in the repository somewhat more tedious. Special care was taken to ensure that the core box inventory sheets were as easy to follow as possible.

The recovered cores will be transported by truck in a refrigerated container to the Gulf Coast Repository. There was one frozen shipment to Stockholm and two shipments were packed with blue ice to go to Santa Cruz and the Pacific Science Center at Vancouver, BC. One set of refrigerated samples was to be picked up and hand carried from the Victoria port call.

The Second Look Lab was cleared of several old and obsolete instruments that were returned to ODP. The lab was set up for resampling cores when necessary. Testing continued on the JANUS database and developmental work continued on the design of a new bin plan for the sample table and a better shipping container for whole-round samples.

Downhole Measurements Lab

Determining the heat-flow characteristics of the area was a major science goal. The measurements were made using the APC Adara tool and the DVTP. In situ temperature measurements were taken 93 times with a 100% success rate. The WSTP pore-water sampler was used twice as an open-hole borehole-water sampler, collecting basement-water samples. It was deployed with the APC/Adara cutting shoe. Any abnormalities in data were the result of formation hardness, drilling problems, leaking thermistors (WSTP), or (possibly) poor instrument calibration (Adara tool 19).

Magnetics Lab

Testing the new cryogenic magnetometer and its software began immediately. The instrument's noise level is low and so far no activity or sea state has had any noticeable effect on the noise level or the liquid helium boil off; the baffles and other improvements have worked well. It is estimated that the next fill will be in 3 years using our current average boil off. Whole-core pass-through capability was restored. A Labview version of the cryogenic magnetometer positioning software was written to replace the problematic software that came with the instrument. No data reduction capabilities were provided.

Routine paleomagnetics tests on Leg 168 were pass-through and discrete measurements for magnetostratigraphy, characterization of magnetic carriers using the pulse magnetizer, and discrete susceptibility measurements and use of the Kappabridge on the basalts.

Aluminum Unistrut framing, which is used to support shelving, was installed around the new cryogenic magnetometer to potentially reduce magnetic fields near the instrument. The capacitors in the GSD-1 demagnetizer were replaced and that instrument was recalibrated.

Paleontology/Microscope Lab

There were few paleontology people this leg, so one of the benches was used by the chemists. One of the centrifuges failed to start; we were unable to locate the schematic that was ordered. One damaged microscope objective was returned for repair.

The state of the chairs in the microscope lab was surveyed and recommendations for new chairs were made. The back support on many is getting weak and the availability of modern mechanisms to easily change seating heights prompted the review.

Photo Lab

While core processing and photography were routine this leg, there were several other photography assignments. Color photographic slides were taken of the labs, equipment, and the CORKs and casing strings. The lab photos of equipment are for the World Wide Web home pages being developed onshore.

Physical Properties Lab

The regular routine of physical properties measurements was performed on the recovered cores and discrete samples were taken. Measurements includes MST, thermal conductivity, Velocity Shear Resistivity (VSR), and index properties.

Thermal conductivity measurements included testing the new Teka thermal conductivity system. The system’s half-space probes seem to be working well and the full-space probes are being tested.

Special projects in the lab included writing control software for the new cryogenic magnetometer in Labview and adding a plotting routine to the MST Process Control screen. The new Moisture and Density (MAD) system was tested. The weighing function did not work correctly. The source code, written in Labview 4.0, was not available.

There was a problem with the balance station that supports the index properties measurements that resulted in using the new sensors from the MAD system. The NB2000 board was installed in a Macintosh IIci to run the balance program. The old sensors’ insidious problem resulted in small errors that were not apparent until the data were processed. The cores were resampled to replace the lost data. The faulty sensors were sent to ODP for repair and recalibration. It is suggested that they be returned to the ship as spares.

A drift in the pycnometer values, $\pm$0.2-0.3 g/cm^3, was traced to a nearly empty (500 psi) helium gas bottle. This was changed and the O-rings replaced, which corrected the problem.

The Thermcon box malfunctioned, resulting in the electronics technicians calibrating the box and needles. The results are being evaluated.

Thin Section Lab

Approximately 63 thin sections were requested. Billets from the last site were taken by the investigators to prepare thin sections at their home institutions. Altered basalt with vesicles and clay was a challenge to work with, requiring epoxy impregnation and occasional duplication.

X-ray Lab

During Leg 168, approximately 700 samples were analyzed by X-ray diffraction. Quantitative analysis was done on most of these samples. MacDiff software was used to calculate peak areas for seven mineral phases and export the results to a spreadsheet. Andy Fisher's revised Pfactor program was then used to derive factors used to determine the percentage of each of the seven minerals in a sample. With the MacDiff software and now the Pfactor program, it is possible to easily, efficiently, and routinely process large numbers of XRD files onboard for quantitative analysis (e.g., Legs 164, 166, and 168).

Twenty-nine basalt samples were analyzed by X-ray fluorescence (XRF) for the usual suite of 10 major element oxides. Because of the chemistry of the new flux (VI), it was necessary to make a set of 14 standard beads for this calibration at a 6:1 flux:standard ratio. Although the standards were weighed on board, the coefficient correlation was excellent and the resulting data were of high quality until near the end of the cruise when goniometer Gonio 2 became unstable again. Problems with the XRF instrument were not resolved in time to do a calibration for trace-element analyses.

With the new flux (VI), it was not possible to make successful bead samples with the previously used 12:1 ratio. The necessacity of using the 6:1 flux:standard ratio resulted in using twice as much sample and some rare standards. The initial change in fluxes lowered the fusing temperature, which created a "less fluffy" physical characteristic that is harder to weigh. Another flux (VII) with a different chemistry was ordered and should have arrived for Leg 169. Some of the initial comparison tests were attempted with the Claisse fluxer, but there were problems with flame stability achieving the fusing temperatures. The NT-2100 bead sampler performed very satisfactorily. The cooling water for it was plumbed to run directly into the eye wash drain.

There were major problems with both goniometers in the XRF instrument. Gonio 1 was not operational. Gonio 2 was operational, but it was not stable over time. When more time became available to work on the unit at the end of the leg, most of the problems were resolved. A service call was scheduled in Victoria to verify the condition of the instrument.

Miscellaneous

Air quality forms were passed out to the science and technical staff to be completed for the use of the Health and Safety Department at Texas A&M University. There have been instances of cruise participants' allergies being aggravated at sea, and this is a step toward systematically investigating these occurrences.

LAB STATISTICS: LEG 168

General Statistics	
Sites	10
Holes	19
Cored Interval (m)	1867.8
Core Recovered (m)	1519.6
Percent Recovered	81.4
Total Penetration (m)	2810.3
Time on Site (days)	47.85
Number of Cores	209
Number of Samples	10507
Whole Rounds	281
Boxes of Core	237
Samples Analyzed	
Inorganic Carbon ($CaCO_3$)	995
Total Carbon (NCHS)	250
Water Chemistry (suite of pH, Alkalinity Sulfate, Calcium, Magnesium, Chlorinity Potassium, Silica, Salinity)	255
Pyrolysis Evaluation (Rock Eval and GHM)	17
Gas Samples	177
Extractions	0
Thin Sections	63
XRF:majors	29
XRD	692
MST Runs	1200
Cryogenic magnetometer	
Pass-through runs	1913
Basalt (210) * 5 levels of demagnetization	1050
Cubes	35
Oriented Cores	0
Physical Properties Velocity	650
Thermal Conductivity	359
Index Properties	650
Resistivity	1796
Shear Strength	470

Under Way Geophysics	
Magnetic (nmi)	670
Bathymetry (nmi)	900
Seismic Survey (nmi)	0
Total Miles (nmi)	1128
XBTs launched	3
Downhole Tools	
WSTP	2
Adara	44
DVTP	49
Additional	
Close-up Photosgraphs	76
Whole-core Photographs	234
Rolls of Microphotographs	10
Color Transparencies	740
Black-and-White Prints	30